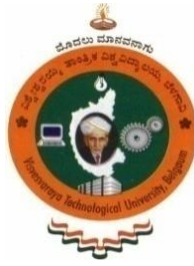


# **B. M. S. COLLEGE OF ENGINEERING, BENGALURU**

An Autonomous Institute, Affiliated to VTU, Belagavi



A Project Report on

## **“Abrasive water jet drilling of Titanium and analysis of hole profile”**

Submitted in partial fulfilment of the requirements for the award of the degree of

**Master in Technology**

In

**MANUFACTURING SCIENCE AND ENGINEERING**

Submitted by:

**HEMANTH L**

**1BM19MSE06**

*Under the guidance of*

**Dr. S SRINIVAS**

Professor

Department of Mechanical Engineering

B. M. S. College of Engineering, Bengaluru-560019



**Department of Mechanical Engineering**

B. M. S. College of Engineering

Bull Temple Road, Basavanagudi, Bengaluru-560019

2020-2021

# CERTIFICATE



## B. M. S. COLLEGE OF ENGINEERING

(An Autonomous Institute, affiliated to VTU, Belagavi)

### Department of Mechanical Engineering

This is to certify that the project report entitled “**Abrasive water jet drilling of Titanium and analysis of hole profile**” submitted by **Hemanth L (1BM19MSE06)**, bonafide student of **B. M. S. College of Engineering**, in the partial fulfilment of the requirement for the award of **Master in Technology in Manufacturing Science and Engineering** of Visvesvaraya Technological University, Belagavi during the year 2020-2021. The project has been approved as it satisfies the academic requirements in respect of the project work prescribed as per the autonomous scheme of B. M. S. College of Engineering for the said degree.

#### Signature of Guide

Dr. S Srinivas  
Professor  
Department of Mechanical Engineering  
B. M. S. College of Engineering  
Bengaluru-560019

#### Signature of the HOD

Dr. Rudra Naik  
Department of Mechanical Engineering  
B. M. S. College of Engineering  
Bengaluru-560019

#### Signature of the Principal

Dr. B V Ravi Shankar  
Principal  
B. M. S. College of Engineering  
Bengaluru-560019

#### NAME OF THE EXAMINER

1.....

2.....

#### SIGNATURE

.....

.....

## DECLARATION

I, Mr. **Hemanth L (1BM19MSE06)**, a student of 4<sup>th</sup> semester in Master of Technology in Manufacturing Science and Engineering, B. M. S. College of Engineering, Bengaluru, hereby declare that the project entitled “**Abrasive water jet drilling of Titanium and analysis of hole profile**” has been independently carried out by me under the guidance of **Dr. S Srinivas**, Professor, Department of Mechanical Engineering, B. M. S. College of Engineering, Bengaluru, in partial fulfillment of the requirements of the degree of Master of Technology in Manufacturing Science and Engineering of Visvesvaraya Technological University, Belagavi.

I further declare that I have not submitted this report either in part or in full to any other university for the award of any degree.

Date:

Hemanth L

Place: Bengaluru

1BM19MSE06

## ACKNOWLEDGEMENT

I would like to convey my sincere gratitude to my guide **Dr. S Srinivas**, Professor, Department of Mechanical Engineering, B. M. S. College of Engineering for his guidance and devoting his time in discussion and giving valuable feedback during project work. I am thankful for his support and motivation.

I extend my sincere thanks to **Dr. Rudra Naik**, Professor & Head, Department of Mechanical Engineering, B. M. S. College of Engineering for his support and valuable suggestions for completion of my project work.

I extend my sincere thanks to **Dr. B. V. Ravi Shankar**, Principal, B. M. S. College of Engineering for his support and valuable suggestions for completion of my project work.

This research work was supported by **Technical Educational Quality Improvement Programme - III**, B. M. S. College of Engineering, Bengaluru, India.

Finally, I would like to thank the college staff and my family who helped me in completing this research work.

## PROJECT SUMMARY

Ti6Al4V is an alpha-beta Titanium alloy with high specific strength and excellent corrosion resistance. They have numerous applications in aerospace, maritime, power generation and requires non-traditional machining for its applications.

The non-traditional machining technique used in this work is abrasive water jet machining. It is a non-traditional machining technique where high pressure and velocity combined with abrasives is used in material removal mechanism. Soft, hard, brittle, ductile and composite materials can be machined using AWJM. This work is focused on the evaluation of performance of the holes drilled in Ti6Al4V by abrasive water jet drilling to understand the effect of cutting parameters such as abrasive flow rate, water jet pressure, drilling time. ANOVA is a mathematical tool which is used to determine the statistical significance of each input parameter, as well as the relative percentage contribution of each parameter to the output parameters and their interactions, as well as to estimate the error variance. This technique was employed to determine the effects of input parameters on output parameters.

Entry Hole Diameter was found to increase with increase in input parameters, that is, abrasive flow rate, water jet pressure, drilling time based on ANOVA results. It was not significantly affected by the interactions between the input parameters and hence was neglected in the formulation of regression equation. Cylindricity was measured for all the 27 holes and it was found that all the holes were within the tolerance limit of 0.1 mm. If the tolerance limit is within 0.025 mm, the deviations obtained in this study does not adhere to it. Hence, for accurately drilling of hole with tolerance limit less than 0.025 mm, abrasive water jet drilling cannot be used for this material. Hole depth was found to increase with increase in input parameters, that is, abrasive flow rate, water jet pressure, drilling time based on ANOVA results. It was significantly affected by the interactions between the input parameters and hence was included in the formulation of regression equation. The SEM images of three different drilled holes are as shown in the images above and the eroded surface is found to be very rough and the eroded particles are not in uniform in their shape and size and when analysed using Energy Dispersive X-Ray Analysis it was found that Titanium, Aluminium and Vanadium had higher weight percentages. This is due to the fact that when material is removed by abrasive water jet, due to raise in localized temperatures in some areas, the eroded particles are adhered to the substrate. The silica elements found during EDX analysis is due to the residue of abrasive particles.

# TABLE OF CONTENTS

Sl No.	Description	Page No.
<b>1</b>	<b>Introduction</b>	<b>1</b>
1.1	Non-Traditional Machining	1
1.2	Abrasive Water Jet Machining	2
1.2.1	Merits and Demerits of Abrasive Water Jet Machining	3
1.2.2	Working of Abrasive Water Jet Machining	5
1.2.2.1	Intensifier Style Pumps	7
1.2.2.2	Direct Drive Pumps	8
1.3	Scanning Electron Microscope	10
1.4	Titanium and its alloys	11
1.4.1	$\alpha$ and near- $\alpha$ alloys	11
1.4.2	$\alpha/\beta$ -alloys	12
1.4.3	$\beta$ -alloys	12
1.5	Ti6Al4V Alloy	12
<b>2</b>	<b>Literature Survey</b>	<b>14</b>
2.1	Summary of literature survey	17
<b>3</b>	<b>Problem Definition and Methodology</b>	<b>18</b>
3.1	Problem Definition	18
3.2	Methodology	18
3.3	Preliminary Experiments	19
3.4	Design of Experiments	20
3.5	Abrasive Water Jet Drilling	21
3.6	Measurement of Output Parameters	23
3.6.1	Measurement of Entry Hole Diameter	23
3.6.2	Measurement of Cylindricity	25
3.6.3	Measurement of Hole Depth	27
<b>4</b>	<b>Results and Discussion</b>	<b>30</b>
4.1	Entry Hole Diameter	30
4.2	Hole Depth	34
4.3	Scanning Electron Microscope	37

4.3.1	SEM and EDX analysis of hole with minimum hole depth	37
4.3.2	SEM analysis of hole with intermediate hole depth	38
4.3.3	SEM and EDX analysis of hole with maximum hole depth	39
4.3.4	Observations from SEM and EDX analysis	41
<b>5</b>	<b>Conclusion</b>	<b>42</b>
	<b>References</b>	<b>44</b>
	<b>Publication Details</b>	<b>45</b>
	<b>Plagiarism Report</b>	<b>64</b>

# LIST OF FIGURES

<b>Sl. No.</b>	<b>Description</b>	<b>Page No.</b>
1.1	Components machined with AWJ	4
1.2	Schematic set-up of Abrasive Water Jet Machine	7
1.3	Intensifier	7
1.4	Working of Direct Drive Pump	8
1.5	AWJM Process	9
1.6	Scanning Electron Microscope	10
3.1	Project Methodology	19
3.2	Abrasive Water Jet Machine	22
3.3	Setup of abrasive water jet drilling of Ti6Al4V	22
3.4	Different of the workpiece after drilling	23
3.5	Profile Projector	23
3.6	Coordinate Measuring Machine	25
3.7	Wire Cut Electric Discharge Machine	27
3.8	Cross section of drilled holes & measurement using Vernier Height Gauge	28
4.1	Main Effects Plot for Entry Hole Diameter	32
4.2	Main Effects Plot for Hole Depth	35
4.3	SEM images of hole drilled with Abrasive flow rate at 200 g/min, Water jet pressure at 15000 psi, drilling time at 120 seconds (Minimum Hole Depth)	37
4.4	EDX spectrum of hole with minimum hole depth	38
4.5	SEM images of hole drilled with Abrasive flow rate at 300 g/min, Water jet pressure at 15000 psi, drilling time at 240 seconds (Intermediate Hole Depth)	39
4.6	SEM images of hole drilled with Abrasive flow rate at 400 g/min, Water jet pressure at 30000 psi, drilling time at 360 seconds (Maximum Hole Depth)	40
4.7	EDX spectrum of hole with maximum hole depth	40



## LIST OF TABLES

Sl. No.	Description	Page No.
1.1	Specifications of Scanning Electron Microscope	10
1.2	Composition of Ti6Al4V alloy	13
3.1	Process Parameters for Abrasive Water Jet Machining	20
3.2	Design of Experiments (L27 Orthogonal Array)	21
3.3	Abrasive Water Jet Cutting Machine Specifications	22
3.4	Specifications of Profile Projector	24
3.5	Values of Entry Hole Diameter	24
3.6	Specifications of Coordinate Measuring Machine	25
3.7	Measurement of Cylindricity	26
3.8	Specifications of Wire Cut Electric Discharge Machine	28
3.9	Values of Hole Depth	29
3.10	Specifications of Scanning Electron Microscope	27
4.1	ANOVA Table for entry hole diameter	30
4.2	Error Analysis of regression equation for entry hole diameter	33
4.3	ANOVA Table for Hole Depth	34
4.4	Error Analysis of regression equation for hole depth	36
4.5	EDX analysis results of hole with minimum hole depth	38
4.6	EDX analysis results of hole with maximum hole depth	41

## TABLE OF ABBREVIATIONS

Abbreviation	Definition
NTM	Non-Traditional Machining
AFR	Abrasive Flow Rate
WJP	Water Jet Pressure
DT	Drilling Time
AWJM	Abrasive Water Jet Machining
AWJD	Abrasive Water Jet Drilling
SEM	Scanning Electron Microscope
EDX	Energy Dispersive X-Ray Analysis
ANOVA	Analysis of Variance

## TABLE OF NOTATIONS

Symbol	Definition
$\dot{m}$	Abrasive Flow Rate
P	Water Jet Pressure
t	Drilling Time

## ***Chapter 1***

# **INTRODUCTION**

## **1.1 Non – Traditional Machining**

Non-traditional machining (NTM) is defined as a machining process in which the material removal mechanism is fundamentally different from traditional processes, i.e., a different form of energy (other than the excessive forces exerted by a tool in physical contact with the work piece) is used to remove excess material from the work surface or to separate the workpiece into smaller parts.

NTM procedures are described as a series of processes that remove superfluous material using a variety of techniques employing mechanical, thermal, electrical, or chemical energy, or combinations of these energies, but do not need the use of a sharp cutting tool as in traditional manufacturing processes. Traditional machining operations such as turning, drilling, shaping, and milling are difficult to use on extremely hard and brittle materials. Typical machining procedures, also known as advanced manufacturing processes, are used when traditional machining processes are not possible, acceptable, or cost-effective for the reasons listed below.

- When the workpiece is too flexible or thin
- When the form of the item is too complicated
- When the workpiece is too hard, brittle, or difficult to clamp for traditional machining

To suit the additional machining criteria, several types of NTM procedures have been created. When used correctly, these processes have several advantages over NTM procedures.

The advantages of NTM are:

- Materials with high value of hardness and strength that are hard to be machined by traditional machining methods can be machined using NTM.
- The workpieces which have low thickness and are too flexible cannot be machined due to lack of support against the cutting forces. These workpieces can be machined using NTM processes.

- 
- The part with intricate geometries, small diameter holes are difficult to be machined and NTM can be used to machine such parts.
  - The surface finish and tolerance obtained from NTM processes are high.
  - Unnecessary generation of heat and temperature rise can be avoided.

The limitations of NTM are:

- Excessive speed of surface generation.
- A combination of chemical and physical events is the base for material removal mechanism in NTM.
- A skilled operator is necessary for the handling of NTM equipment.
- The initial investment cost and processing cost for NTM processes are high.
- It is not economical for batch and mass production.

## 1.2 Abrasive Water Jet Machining

Water Jet Machining (WJM) is a mechanically enhanced NTM technique in which a high-velocity stream of water is used to erode tiny parts of the workpiece's surface. In the early 1970s, WJM was first utilized for soft material cutting, cleaning, and coating removal. This method was used to cut softer materials including wood, plastic, and rubber. It hasn't had any issues with vibrations. Another machining technology known as Abrasive Water Jet Machining (AWJM) was developed to machine hard materials such as metals and granite.

AWJM is an NTM process that achieves outcomes by combining the efforts of AJM and WJM to overcome the disadvantages of each separate procedure. It improves and expands WJM's capacity to machine hard or tough materials. In AWJM, a high-velocity jet of water is combined with abrasive particles to boost the process' efficiency in terms of material removal rate and the ability to cut all materials (no matter hard or soft). When high-velocity water collides with tiny abrasive particles on the workpiece, the material is eroded by impact. Because there are no heat impacts, this technique is ecologically benign and has no influence on the materials' characteristics (or internal structure). WJM and AWJM are both contemporary machining techniques that leave no heat impacted zone or residual stress on the machined surface or workpiece.

The following is the main concept involved in the material removal process: Water is pumped from a reservoir to an intensifier using a hydraulic pump. In the intensifier, the

---

water pressure is boosted to the required amount. Water is often compressed to a pressure of 200 to 400 MPa. The pressurized water is subsequently received by the accumulator, which temporarily stores it. The pressured water enters the nozzle through the flow regulator and control valve. The flow rate of water is managed by the flow regulator, while the direction and pressure of water are controlled by the control valve. When pressurized water enters through orifice, its kinetic energy skyrockets, resulting in an extremely high-velocity water jet. As the water jet hits and strikes the workpiece's surface, stress is created on the workpiece. These forces operate on the workpiece surface, removing material without forming a Heat Affected Zone.

### **1.2.1 Merits and Demerits of Abrasive Water Jet Machining**

The advantages of AWJM technique are:

- Water is inexpensive, non-toxic, readily available, and easily discarded. It is an environmentally beneficial technique since no harmful gases are created.
- Because there is no heat affected zone, it may manufacture workpieces without leaving any mechanical strains or changes in the microstructure of the workpiece.
- With a great surface polish and a generally clean and dust-free environment, complex geometries and complicated cuts may be easily performed.
- AWJM may be used to machine both hard, soft and thick materials.
- The machining precision is good. Tolerances of the order of 0.005 inch are easily achievable.
- Three Dimensional Cutting is possible.

The limitations of AWJM are as follows:

- The equipment is extremely pricey, resulting in a prohibitively large initial expenditure. It is inappropriate for batch manufacturing due to its high cost.
- While it is feasible to machine hard materials, doing so successfully (with the needed precision and surface polish) necessitates a significant reduction in material removal rate, hence increasing the time required for each cut.
- Very thick materials cannot be machined with the precision necessary; in such circumstances, the energy of the water jet dissipates, resulting in a larger cut at the bottom of the workpiece than at the top.

- When many pieces are cut from a single blank, the thin kerf enables for tight nesting.
- During machining, the AWJM process generates a lot of noise.
- At the bottom of the cut, striations are made.

AWJM can also be applied in other areas such as removal of paint, peening to reduce residual stress, cleaning. AWJM could also be used in pocket milling, drilling and turning operations. Some of the components that can be machine using AWJM is as shown in figure 1.1.



**Fig. 1.1 Components machined with AWJ**

---

### 1.2.2 Working of Abrasive Water Jet Machining

Figure 1.2 depicts a schematic layout of the AWJM. The procedure necessitates the use of many pieces of equipment or units, including:

#### (I) Hydraulic Pump Unit

The primary goal of this machine is to convert momentum from a high-pressure water jet to abrasive particles, which, when struck by a workpiece, induce material removal. It is made up of five sub-components:

**a) Electric motor:** The hydraulic pump is driven by an electric motor with an usual capacity of 20 to 75 HP.

**b) Hydraulic pump:** The pump is driven by an electric motor, which generates hydraulic pressure in the range of 15–30 MPa. Hydraulic intensifier pumps and crankshaft pumps are the two most common types. When compared to the hydraulic intensifier pump, the crankshaft pump is more efficient and hence achieves quicker cutting.

**c) Intensifier:** Because the Intensifier employs a bigger oil piston than a typical water piston, the water pressure is boosted to more than 40 times the hydraulic pressure. The square of the diameter ratio of an oil and water piston is equal to hydraulic pressure divided by water pressure. Water pressure may be readily controlled by adjusting the lower pressure oil.

**d) Accumulator:** The accumulator temporarily stores the high-pressured water until a large amount of pressure energy is required. The fluid is then delivered to remove any pressure changes, resulting in a consistent water flow at the outlet.

**e) Tubing:** A vacuum chamber called tubing is used to combine water and abrasive particles. Flexible tubing is preferable at pressures up to 24 MPa, however stiff tubing is also used.

#### (II) Water Feeding Unit

An orifice is used to force pressurised water (500 MPa) through a nozzle, resulting in a 900m/s water jet. Units are comparable in both the WJM and AWJM approaches. The nozzle of a water jet is made of synthetic sapphire and tungsten carbide.

### **(III) Abrasive Feed Unit**

A hopper and flow control system within the feed unit send abrasive particles to the nozzle in a controlled and exact way. There are primarily two particle delivery methods:

- a) Dry abrasive delivery:** It is appropriate when the delivery distance is short.
- b) Abrasive slurry feed:** Particles may be introduced across a long distance, however this technology takes more power each cut, and commercial availability is restricted.

### **(IV) Abrasive Water Jet Nozzle**

A device known as a Nozzle can be used to regulate the properties and direction of a fluid's flow as it exits a pipe. After converting high-pressure water into high-velocity water, it emerges through the nozzle. Water and abrasives are extensively mixed here to make a cohesive combination. The two main configurations that have been modified are:

- a) Single-jet side feed:** The water jet is positioned in the centre, while abrasives are applied to the water jet's periphery. This arrangement is quite simple to manufacture. It, on the other hand, does not enable proper mixing of the water jet with the abrasives and wears out more quickly, making it less attractive.
- b) Multiple-jet central feed:** Abrasives are injected in the centre, with several water jets added on the abrasive jet's periphery. It provides optimal mixing and longer nozzle life, but it is more expensive and complex to manufacture. Computer-based motion controllers are used to regulate the nozzle's movement.

### **(V) Worktable**

Accurate cutting is guaranteed by employing computer numerical control systems to provide easy and exact motion to the abrasive water jet nozzle relative to the workpiece along all three axes. Worktables come in a variety of forms and sizes, ranging from little to extremely large, and may be customised to meet your needs.

### **(VI) Drain and Catcher System**

The energy of the abrasive water jet is dispersed here to decrease noise and prevent the jet from leaving the workpiece.



- A catcher is utilised when the abrasive water jet nozzle is at rest and the workpiece is in motion (moving).
- A settling tank is utilised when the abrasive water jet nozzle is in motion (moving) and the workpiece is at rest.

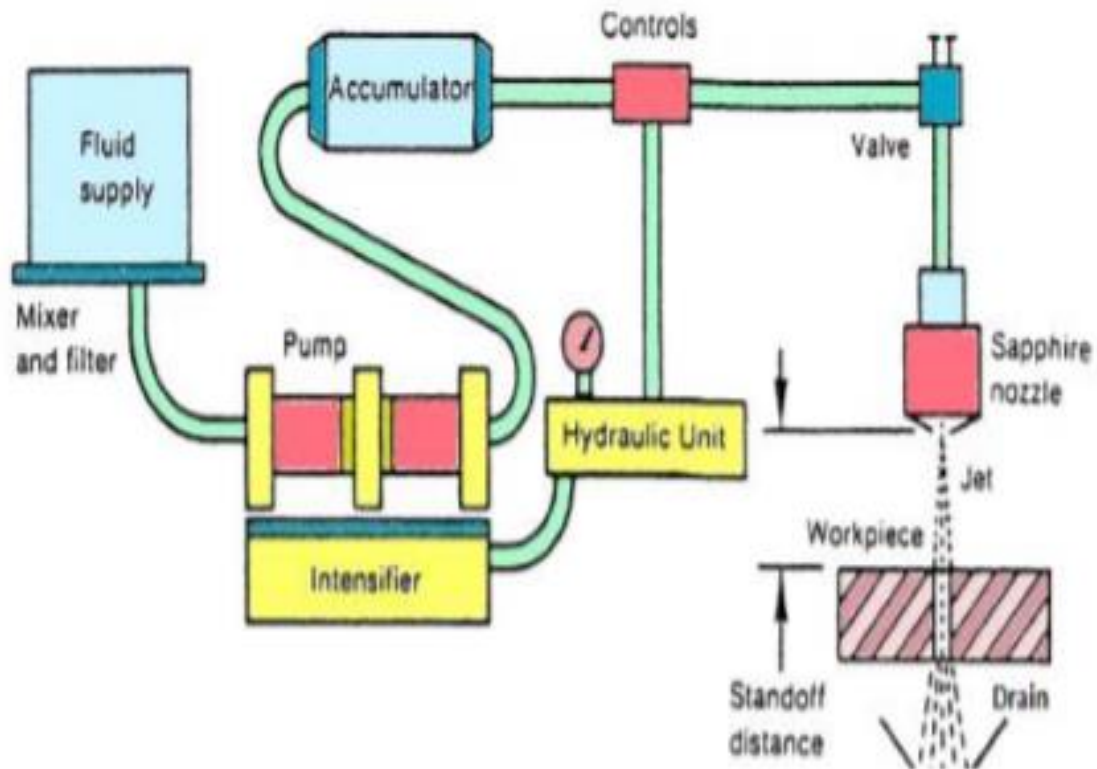


**Fig. 1.2 Schematic set-up of Abrasive Water Jet Machine [1]**

### 1.2.2.1 Intensifier Style Pumps

The intensifier is as depicted in Figure 1.3 and is guided with the help of a positive displacement hydraulic pump. The hydraulic pumps are administered by microcomputers to accomplish the programmed rise in pressure etc.

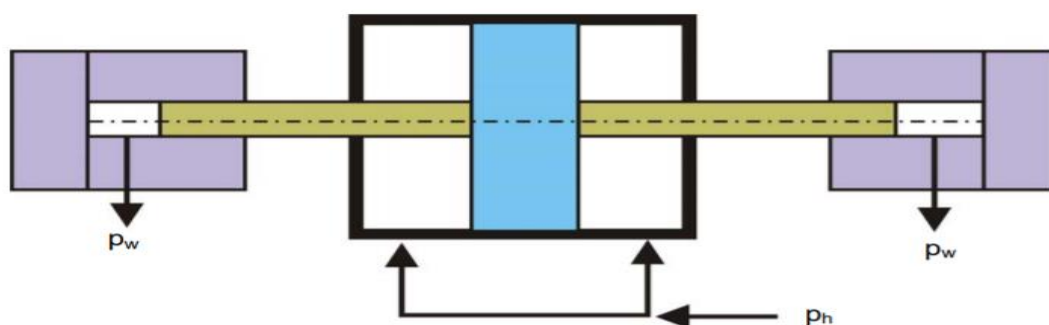


**Fig. 1.3 Intensifier [1]**

With the help of direction control valve, the hydraulic unit guides the intensifier. The water to the intensifier could be supplied directly or by a booster which assists in increasing the water pressure before it is supplied to the intensifier. Hence, high pressure water is delivered with the help of intensifier. To oppose the change in pressure which occurs due to changes in direction of the piston within the intensifier, a thick cylinder known as the accumulator is attached for storing water at high pressure. It minimizes the water pressure fluctuation and often acts as a flywheel of an engine.

### 1.2.2.2 Direct Drive Pumps

The direct drive pump is as shown in figure 1.4. The working of direct drive pump is similar to that of a car's engine. A crankshaft is turned with the help of a motor. This crankshaft is connected to three or more pistons. The motor turns the crankshaft and pressure is created in the water due to reciprocating motion of the piston in their cylinders. The speed by which the motor turns the determines the WJP and AFR. There is no need of an attenuator in the case of direct drive pumps. The AWJM in this research follows this mechanism.

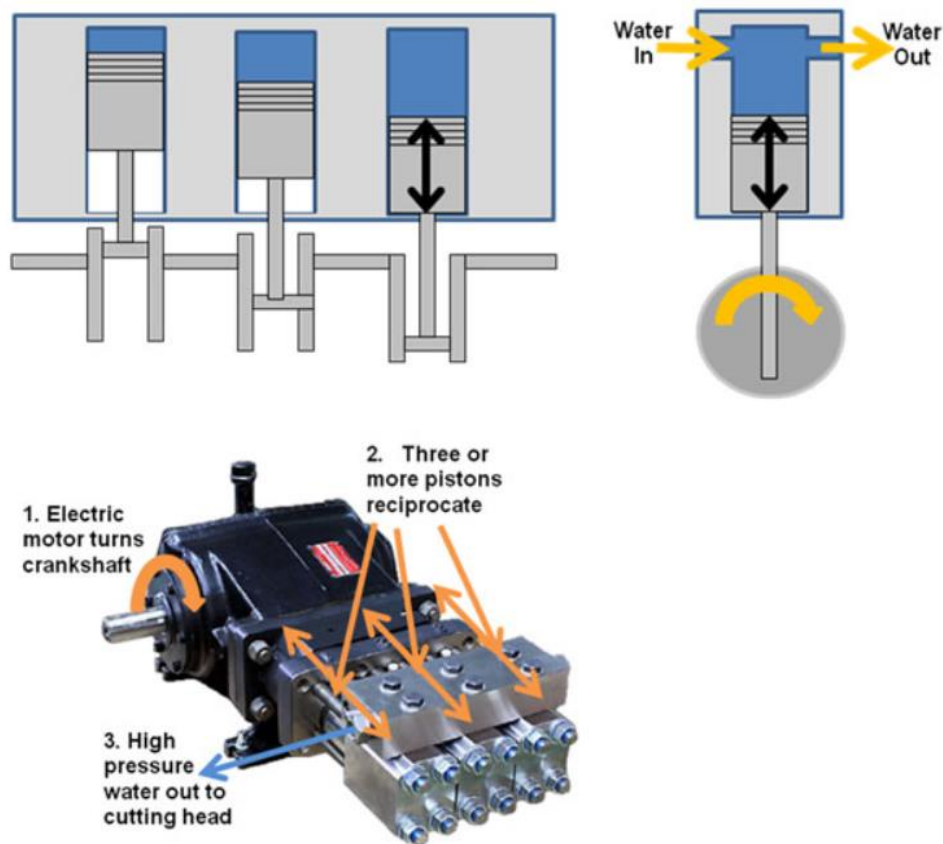


**Fig. 1.4 Working of Direct Drive Pump [1]**

The intensifier converts low-pressure water into high-pressure water at a pressure between 3000 and 4000 bar (300MPa to 400MPa). Both the accumulator and the nozzle get this high-pressure water. The high-pressure water is stored in the accumulator and delivered as needed. It is used to reduce high-pressure demand fluctuation while cutting hard materials. The high-pressure water is then directed to the nozzle, where the high-pressure energy of water is transformed to high kinetic energy of water (water expands with a significant rise in its kinetic energy or velocity), resulting in a narrow beam of extremely high-velocity water leaving the nozzle.

Within the nozzle, abrasive particles such as garnet, olivine, or aluminium oxide are combined with water. The nozzle has a mixing chamber where the abrasives are combined with the high-velocity water in either single-jet side feed or multi-jet central feed variants. When the high-velocity water jet emerges from the nozzle and meets the workpiece, it removes material by erosion, stress produced on the workpiece, and fracture of tiny pieces of the workpiece at the contact site. After machining, the water jet is collected by the drain and catcher system. The trash and metal particles from the water are removed here, and the water is then sent to the reservoir tank. The AWJM process is as shown in figure 1.5. This is how the complete material removal procedure is carried out with Abrasive Water Jet Machining.

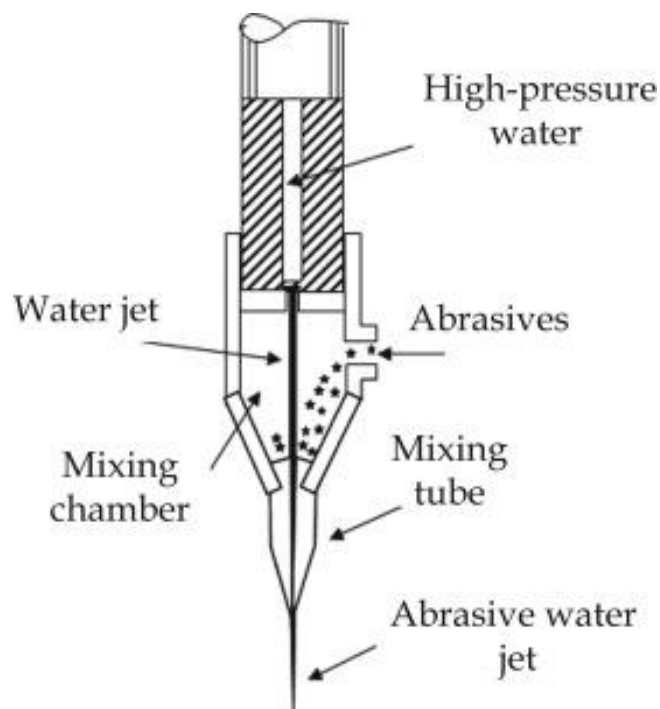


**Fig 1.5 AWJM Process**

### 1.3 Scanning Electron Microscope

A scanning electron microscope (SEM) is a sophisticated microscope that uses a stream of electrons to scan the surface of a workpiece and generate pictures. The interaction of electrons and atoms in the workpiece produces a range of signals that provide information on the sample's composition and topography. The electron beam scans the sample in a raster scan pattern, and the position of the electron beam, together with the strength of the received signal, aids in picture generation. The scanning electron microscope is as shown in Figure 1.6



**Figure 1.6 Scanning Electron Microscope**

The specifications of the scanning electron microscope are as shown in the table 1.1.

**Table 1.1 Specifications of Scanning Electron Microscope**

<b>Make</b>	TESCAN-VEGA 3 LMU
<b>Resolution</b>	3 nm at 30 kV
<b>Magnification</b>	Continuous from 4.5 X to 1,000,000X
<b>Maximum Field of View</b>	0.08 $\mu\text{m}$
<b>Accelerating Voltage</b>	200 V to 30kV
<b>Electron Gun</b>	Tungsten Heated Cathode
<b>Probe Current</b>	1 pA to 2 $\mu\text{A}$
<b>Scanning Speed</b>	From 20 ns to 10 ms per pixel
<b>Image Size</b>	Upto 8192x8192 pixels in 32-bit quality

## 1.4 Titanium and its alloys

Titanium is a desirable material for aerospace applications, but it has been limited in usage owing to cost concerns. It has a strong strength-to-weight ratio, good corrosion resistance, and cryogenic and extreme temperature characteristics. However, its beginning prices might be 5–10 times more than aluminium or high-strength low-alloy (HSLA) steel alloys, and machining costs could be 2 orders of magnitude higher than Al alloys. As a result, Ti uses on commercial aircraft structures have been limited - each application must be justified in terms of cost vs better performance or lower maintenance expenses. Military aircraft may face a different dilemma, since larger expenses per kilogramme of weight saved are frequently easier to justify due to their increased focus on performance. Following are the advantages of Ti alloys

- **Reduced Weight**
- **Operating Temperature** – Titanium alloys are employed at a broad variety of temperatures, including cryogenic temperatures (252°C) for rocket engines and continuous working temperatures as high as 600°C for gas turbine engines.
- **Space Limitations** – Some constructions have limited areas, which necessitate the usage of titanium.
- **Corrosion Resistance** – Titanium is almost impervious to the materials it comes into contact with in an aircraft environment. When a new Ti surface is exposed to air, a thin, nascent, persistent oxide layer forms almost immediately, providing corrosion resistance.
- **Composite Compatibility** – Although this is linked to corrosion resistance, it is thought that it warrants its own explanation. In an aqueous solution, Ti is compatible with graphite fibres in the polymeric composites that are widely employed today, but Aluminum (Al) and high strength low alloy (HSLA) steels would form a galvanic cell, resulting in metal corrosion.
- **Low Modulus** – Ti alloys' low shear modulus and strong yield strength, along with their low density, make them ideal spring materials.

### 1.4.1 $\alpha$ and near- $\alpha$ alloys

As one might expect, these alloys are predominantly, with a little amount of  $\beta$ -phase (up to a few percent) present.

Even in economically pure Ti, some  $\beta$ -phase is usually always present. Although O<sub>2</sub> is the major alloying element in commercially pure steel, Fe (0.2 to 0.4 percent) is always added to offer extra strength and increase both workability and hydrogen tolerance. (Composition percentages are always expressed as a proportion of total weight.) Near-alloys, such as Ti-6Al-2Sn-4Zr-2Mo (Ti6242), are commonly used in high-temperature applications.

### 1.4.2 $\alpha/\beta$ -alloys

The area between the boundary of the  $\alpha$  - alloys and the metastable  $\beta$  - alloys is characterised as this class of alloys – martensite is generated when quenching from temperatures in the  $\alpha + \beta$  phase field or above. They include anything from a few percent to large levels of  $\beta$ -stabilizer, but not enough to keep 100 percent at ambient temperature.

### 1.4.3 $\beta$ -alloys

These alloys, which include above 10%–12%  $\beta$  -stabilizing alloying additives, may be solution treated above the  $\beta$  temperature, cooled to room temperature, and still preserve 100%  $\beta$ -phase. Some alloys, such as Ti-10V-2Fe-3Al, require water quenching to achieve this, although more heavily-stabilized alloys, such as Ti-15V3Cr-3Al-3Sn and Ti-3Al-8V-6Cr-4Zr-4Mo, may be able to do this with air cooling, particularly for thinner gauges. Though they are commonly referred to as  $\beta$  -alloys, the commercial alloys utilized in the aircraft industry are all metastable  $\beta$  -alloys.

## 1.5 Ti6Al4V Alloy

The titanium industry's workhorse alloy is this alpha-beta alloy. The alloy is completely heat treatable in sections up to 15mm and can withstand temperatures of up to 400°C (750°F). Its usage encompass various aerospace airframes and engine component uses, as well as large non-aerospace applications in the marine, offshore, and power generation sectors in particular, because it is the most often used alloy – over 70% of all alloy grades melted are a sub-grade of Ti6Al4V. In reducing acid, chloride, and sour environments, the addition of 0.05 percent palladium (grade 24), 0.1 percent ruthenium (grade 29), and 0.05 percent palladium and 0.5 percent nickel (grade 25) significantly increases corrosion resistance, raising the attack temperature to well over 200°C (392°F).

This is the most often used titanium alloy. It's employed in a variety of sectors, including aerospace, maritime, power generating, and offshore. The composition of Ti6Al4V is as shown in Table 1.2.

**Table 1.2 Composition of Ti6Al4V alloy [2]**

<b>Material</b>	<b>Percentage</b>
Carbon	0.08 %
Iron	0.25 %
Nitrogen	0.05 %
Oxygen	0.20 %
Aluminium	6.25 %
Vanadium	4.00 %
Hydrogen	0.01 %
Titanium	Balance

---

## Chapter 2

### Literature Review

**Huaizhong Li & Jun Wang. [3]** experimentally studied abrasive waterjet (AWJ) machining of the most commonly used titanium alloy, Ti-6Al-4V. Two types of machining operations, i.e. drilling (or piercing) and slotting, were conducted. For the drilling experiments, the influences of water pressure and drilling time were investigated. It was found that both the hole depth and diameter increased as drilling time increased but in a decreasing rate. An increase in the water pressure increased both the hole depth and the hole diameter. For the slot cutting, the influence of water pressure and the traverse speed were investigated. A slower traverse speed resulted in a deeper depth of cut. The kerf showed a taper shape with a wider entry on top, and the width decreased as jet cut into the material. At the bottom of the kerf, a pocket was generated. The variation of the depth of cut became insignificant when the traverse speed was increased.

**Jegaraj and Babu [4]** carried experimental studies to investigate the influence of orifice and focusing tube bore variation on the performance of abrasive waterjets in cutting 6063-T6 aluminum alloy. The performance was assessed in terms of different parameters such as depth of cut, kerf width and surface roughness. This study made use of Taguchi's design of experiments and analysis of variance (ANOVA) to analyze the performance of AWJs in cutting. These experimental data was used to build empirical models. An hybrid strategy combining the response equations of the empirical model with fuzzy model is proposed to arrive at suitable set of process parameters for achieving desired cutting performance considering the variation in orifice and focusing tube bore. The adequacy of the model is confirmed with suitable experiments.

**J Wang et al [5]** presented a computational model is to investigate the ultrahigh-velocity multiple particle impact process on steels. It uses a Monte Carlo framework to model the stochastic nature of the particle flow and the finite element (FE) method to model the individual particle impact process, while considering the thermal diffusion process. The model predictions show a reasonably good agreement with the corresponding experimental data using a high-tensile steel specimen at various conditions. A simulation study using the model is then conducted and shows that it is essential to consider thermal diffusion which causes the temperature at the impact site to rapidly cool down in a multiple particle impact process. As a consequence, the impact result is impact-sequence and impact-time

---



dependent. The study reveals that inertia-induced fracture is the primary material removal mechanism at the normal impacts, while the thermal instability-driven failure, or specifically the adiabatic shear banding (ASB) induced failure, as well as the elongation-induced fractures are the two major material removal mechanisms at oblique impact angles. These failures occur at the pile-up lips (at normal and oblique impact angles) and the crater bottom (at oblique impact angles). It is the thermal-instability-driven failure that contributes to the higher material removal rate at oblique impact angles

**Caydas and Hascalik [6]** studied and developed artificial neural network (ANN) and regression model to predict surface roughness in abrasive waterjet machining (AWJ) process. In the development of predictive models, machining parameters of traverse speed, waterjet pressure, standoff distance, abrasive grit size and abrasive flow rate were considered as model variables. For this purpose, Taguchi's design of experiments was carried out in order to collect surface roughness values. A feed forward neural network based on back propagation was made up of 13 input neurons, 22 hidden neurons and one output neuron. The 13 sets of data were randomly selected from orthogonal array for training and residuals were used to check the performance. Analysis of variance (ANOVA) and F-test were used to check the validity of regression model and to determine the significant parameter affecting the surface roughness. The statistical analysis showed that the waterjet pressure was an utmost parameter on surface roughness. The microstructures of machined surfaces were also studied by scanning electron microscopy (SEM). The SEM investigations revealed that AWJ machining produced three distinct zones along the cut surface of AA 7075 aluminium alloy and surface striations and waviness were increased significantly with jet pressure.

**R. Ronaldo et al [7]** presented a new approach called spindle-peak-frequency (SPF) for determining stable microdrilling parameters. The novelty is that the approach does not require a force model, material behaviour of the workpiece, modal stiffness and damping of the drilling tools. The only required parameter is the natural frequency of the drilling tools, which is obtained by modal dynamic finite element analysis (FEA). Material constants for the Johnson–Cook material model for Macor are obtained and implemented into a FE model of orthogonal cutting to investigate the cutting mechanisms. The results have shown that the cutting mechanisms of the Macor are achieved by initiation and propagation of micro-cracks. Finally, the developed research methods have been implemented to manufacture Macor nozzles of scanning droplet systems where holes with

diameter of 100  $\mu\text{m}$  and aspect ratio of 10 have been successfully drilled which has increased the resolution by 5 times.

**Alberdi et al. [8]** studied CFRP/Ti6Al4V stacks that were machined with abrasive water jet using different process parameters in order to evaluate the viability of AWJ industrial application as a substitute of conventional drilling. The effect of the stack configuration, the traverse feed rate, the cutting tool (combination of orifice and focusing tube diameter and abrasive mass flow rate), and the pressure over the kerf profile, taper angle, and surface roughness has been analyzed through an ANOVA analysis and related to the physical parameters of the AWJ process. As a result, a positive taper angle is observed in Ti6Al4V while a negative is observed in CFRP in almost all cutting conditions. This leads to obtain an X-type or barrel-type kerf profile depending on the stack configuration. In addition, the surface roughness can be as low as 6.5  $\mu\text{m}$  in both CFRP and Ti6Al4V materials at 95 mm/min when CFRP/Ti6Al4V configuration is used.

**Gault R et al. [9]** experimentally studied stacks composed of titanium and carbon-fibre-reinforced polymer (CFRP) with the aim to investigate the effect of water-jet process variables on drilled diameter and surface condition. A design of experiments approach was taken, considering variables such as water pressure, traverse rate, abrasive mass flow and stack set-up. Two different set-ups were investigated: CFRP over titanium (CFRP/Ti) and vice versa (Ti/CFRP). The experimental variables were related to taper ratio, surface roughness of the hole bore, hole quality and surface condition. Statistical analysis was carried out in order to develop mathematical models which include process variables interactions and quadratic terms. This led to models with high correlation and prediction power; which allow a better understanding of the process and can form the base for further process optimisation. The models were validated with additional experiments and showed good agreement with the water-jet system. The results showed that set-up and its interaction with other process variables has a strong influence on the performance of the abrasive water-jet system.

**Chang and Kuo [10]** While drilling a hole in titanium alloy, researchers looked at the surface roughness and material removal rate. During the testing, they changed the rotation speed, feed, depth of cut, and pulse frequency and discovered that the rotational speed was the most important factor impacting both the surface roughness and material removal rate

---

## 2.1 Summary of Literature Review

- It was found that various researchers worked on abrasive water jet drilling of different materials with different process parameters.
- The process parameters obtained from literature review were: standoff distance, abrasive concentration, jet pressure, drilling time, abrasive flow rate.
- The output parameters obtained from literature review were: material removal rate, surface roughness, depth of cut, entry hole diameter, exit hole diameter, entry hole roundness, exit hole roundness, kerf width, measure circularity and cylindricity, Scanning Electron Microscopy (SEM) to observe the chipping and cracks developed during machining.
- According to the current literature review, there has been little work done in the field of employing AWJ to drill Titanium alloy, and there is scope to investigate the hole profile with full factorial trials. As a result, the focus of this research was on using AWJ to drill Ti6Al4V and analysing the hole profile.
- Process parameters selected as per literature review: Water jet pressure, Abrasive Flow rate, Drilling Time.
- Output parameters selected as per literature survey: Measurement of Entry Hole Diameter, Measurement of Hole Depth, Measurement of cylindricity, microstructural study.

---

## **Chapter 3**

# **PROBLEM DEFINITION AND EXPERIMENTAL PROCEDURE**

## **3.1 Problem Definition**

The objective of the present work is to experimentally study the “**Abrasive water jet drilling of Titanium and analysis of hole profile**”.

## **3.2 Methodology**

To attain the main objectives of the project, the experimental work was carried out in the following sequence as depicted in figure 3.1.

- Procurement of the selected material – Ti6Al4V (Titanium Alloy)
- Decision of values for process parameters used for machining based on the results and observations from preliminary experimentation and design of experiments  
Since there are three factors and each factor has three levels,  $3^3 = 27$  experiments will be performed based on Taguchi’s orthogonal array ( $L_{27}$ )
- Measurement of output parameters
  1. Measurement of entry hole diameter using profile projector
  2. Measurement of cylindricity of hole using coordinate measuring machine.
  3. Measurement of hole depth using Vernier Height Gauge.
  4. Characterization of hole profile using Scanning Electron Microscope.
- Results and Discussion.
  1. ANOVA to determine the significant factors.
  2. Effect of significant factors on the output parameters.
- Paper and Report writing

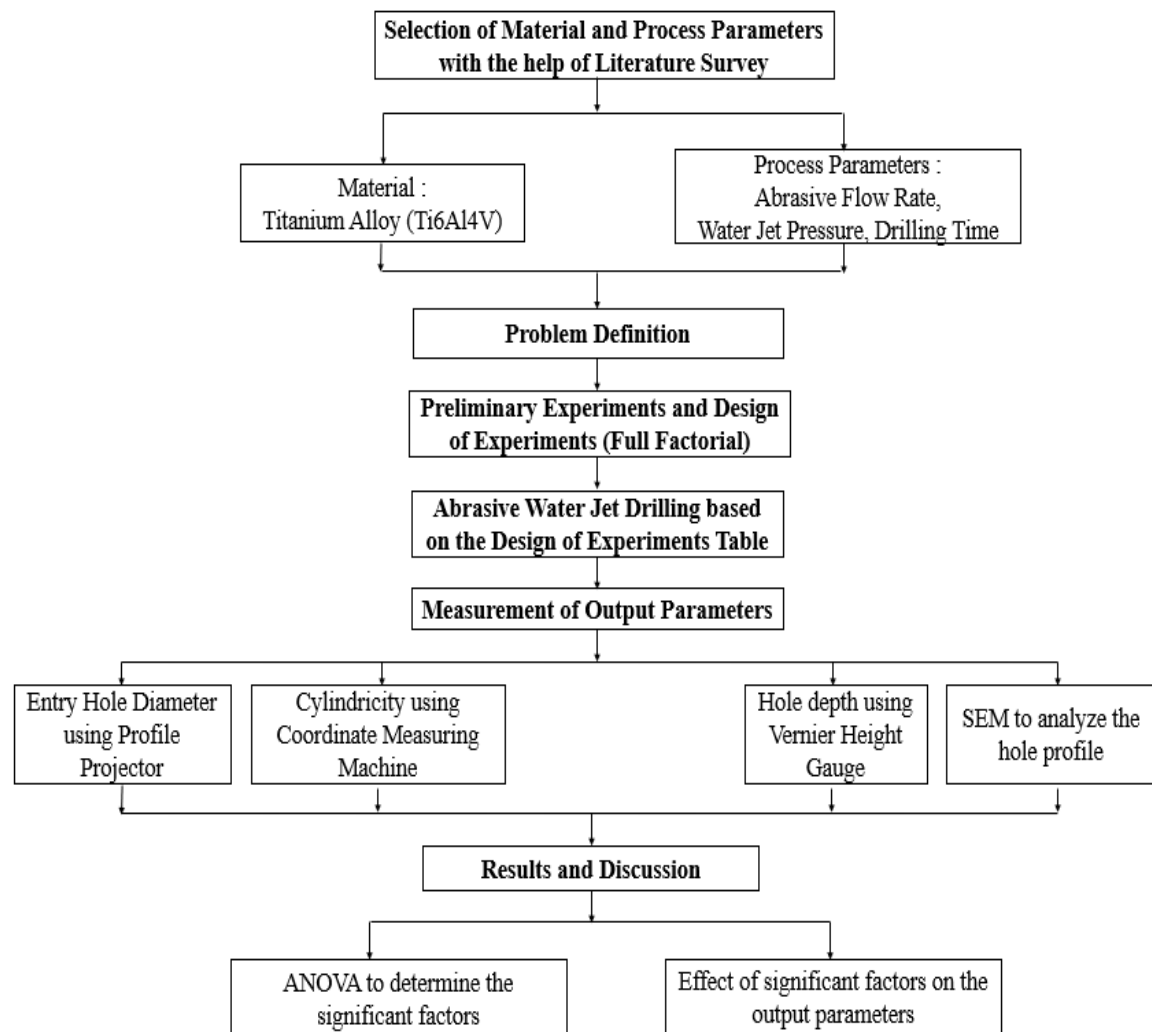


**Fig. 3.1 Project Methodology**

### 3.3 Preliminary Experiments

In the preliminary experiments phase, through holes at minimum and maximum specifications of the abrasive water jet machine were drilled and the time taken for both the specifications was measured.

- **At maximum specification**
  - ❖ Pressure = 30000 PSI
  - ❖ Flow rate = 400 g/min

The time taken was **4 minutes and 2 seconds**.

Based on the minimum specifications of the machine and preliminary experiments the levels for three factors were determined.

Water Pressure (psi) – 15000, 22500, 30000

Abrasive Flow Rate (g/min) – 200, 300, 400

Drilling Time (s) – 80, 140, 200

**Table 3.1 Process Parameters for AWJM**

<b>Factors</b>	<b>Level 1</b>		<b>Level 2</b>		<b>Level 3</b>	
Water Jet Pressure (psi)	(I)	15000	(II)	22500	(III)	30000
Abrasive Flow Rate (g/min)	(A)	200	(B)	300	(C)	400
Drilling Time (s)	(i)	80	(ii)	140	(iii)	200
Standoff Distance (mm)	3					
Abrasive Mesh size	80					
Orifice Diameter (mm)	0.25					
Focusing nozzle diameter (mm)	1.07 and material is Tungsten Carbide					
Abrasive Material	Garnet					
Impact Angle	90°					

### 3.4 Design of Experiments

Experimental design is found to be a very useful strategy for accomplishing derivation of conclusions which are clear and accurate from the experimental observations.

Three levels and three factors are considered in the present research work. The full factorial design of experiments was employed for this case.

$$(\text{Level})^{\text{Factor}} = (3)^3 = 27.$$

Hence, full factorial  $L_{27}$  orthogonal array was chosen and the experiments are designed and tabulated.

The tabular column of design of experiments is as shown table 3.2:

**Table 3.2 Design of Experiments (L<sub>27</sub> Orthogonal Array)**

<b>Sl. No.</b>	<b>Abrasive Flow Rate (g/min)</b>	<b>Water Pressure (psi)</b>	<b>Drilling Time (s)</b>
1	200	15000	80
2	200	15000	140
3	200	15000	200
4	200	22500	80
5	200	22500	140
6	200	22500	200
7	200	30000	80
8	200	30000	140
9	200	30000	200
10	300	15000	80
11	300	15000	140
12	300	15000	200
13	300	22500	80
14	300	22500	140
15	300	22500	200
16	300	30000	80
17	300	30000	140
18	300	30000	200
19	400	15000	80
20	400	15000	140
21	400	15000	200
22	400	22500	80
23	400	22500	140
24	400	22500	200
25	400	30000	80
26	400	30000	140
27	400	30000	200

### 3.5 Abrasive Water Jet Drilling of Titanium

Table 3.2 shows how experimental values as per full factorial design. Figure 3.2 depicts the equipment used for abrasive water jet drilling. The abrasive water jet machine's important specifications are provided in table 3.3. The OMAX Corp. WA USA Abrasive Water Jet Cutting Model – MAXIEM 1515 was used for experimentation.

The setup of abrasive water jet drilling of Ti6Al4V is as shown in the figure 3.3.



**Figure 3.2 Abrasive Water Jet Machine**

**Table 3.3 Abrasive Water Jet Cutting Machine Specifications**

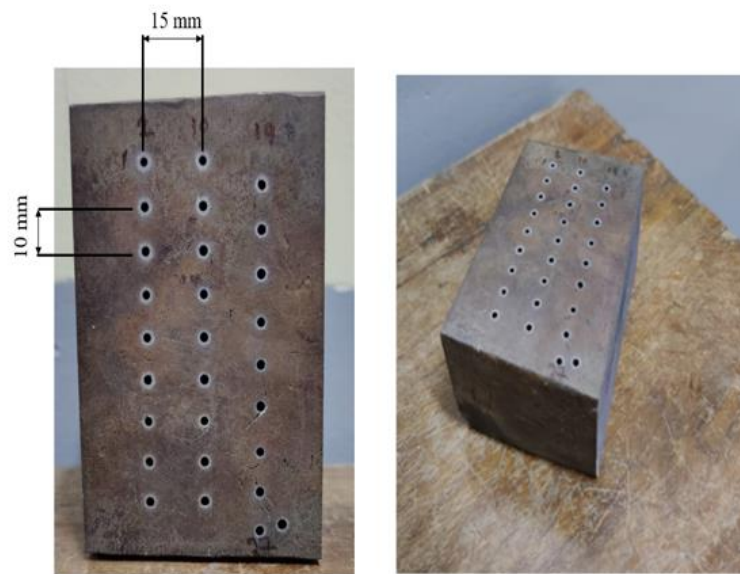
<b>Make</b>	OMAX Corp. WA USA– MAXIEM 1515
<b>X – Y Travel</b>	1575 x 1575 mm mm
<b>Z Travel</b>	150 mm
<b>Cutting Head</b>	5 Axis machining up to 59° taper
<b>Traverse Speed</b>	8000 mm/min
<b>Pressure</b>	15000 – 30000 psi



**Figure 3.3 Setup of abrasive water jet drilling of Ti6Al4V**



The front and isometric views of the workpiece after the drilling process is as depicted in the figure 3.4.



**Front View of the Workpiece    Isometric View of the Workpiece**

**Figure 3.4 Different views of the workpiece after drilling**

## 3.6 Measurement of Output Parameters

### 3.6.1 Measurement of Entry Hole Diameter

The diameter of the drilled hole at the workpiece's surface is the entrance hole diameter. It was measured using the Nikon Profile Projector (V-24B). The profile projector and its specifications are as depicted in figure 3.5 and table 3.3.

The values of the entry hole diameter are measured and tabulated as shown in table 3.5

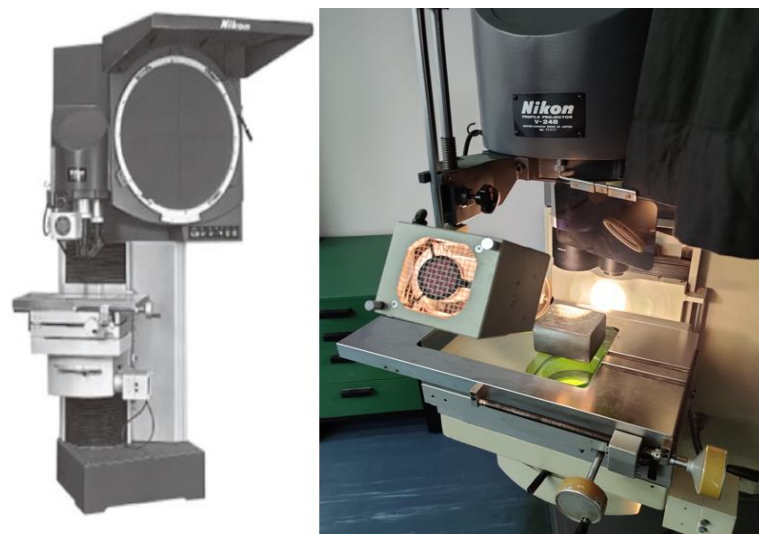


**Figure 3.5 Profile Projector**

**Table 3.4 Specifications of Profile Projector**

<b>Make</b>	Nikon V-24 B
<b>Type</b>	Vertical optical axis
<b>Image</b>	Inverted and reversed
<b>Screen</b>	Φ600 mm; etched centre crossline; 1-minute protractor; incline 4 off vertical
<b>Lens mount</b>	3-lens turret mount; screw type
<b>Projection lens</b>	5x, 10x, 20x, 50x, 100x
<b>Magnification Accuracy</b>	0.05% for contour illumination; 0.075% for surface illumination
<b>Light Source</b>	24V-150W halogen for both contour and surface illumination
<b>Max. workpiece height</b>	250 mm
<b>Stage</b>	9V Stage directly mountable
<b>Power Input</b>	AC 100-120V (CSA), 220-240V (CEE), 240V (SAA)
<b>Dimensions (WxDxH)</b>	1180x1100x1900 mm

**Table 3.5 Values of Entry Hole Diameter**

<b>Sl. No.</b>	<b>Abrasive Flow Rate (g/min)</b>	<b>Water Pressure (psi)</b>	<b>Drilling Time (s)</b>	<b>Entry Hole Diameter (mm)</b>
1	200	15000	120	1.909
2	200	15000	240	2.024
3	200	15000	360	2.136
4	200	22500	120	1.957
5	200	22500	240	2.078
6	200	22500	360	2.184
7	200	30000	120	2.044
8	200	30000	240	2.124
9	200	30000	360	2.282
10	300	15000	120	1.942
11	300	15000	240	2.125
12	300	15000	360	2.191
13	300	22500	120	2.035
14	300	22500	240	2.110
15	300	22500	360	2.251
16	300	30000	120	2.090
17	300	30000	240	2.194
18	300	30000	360	2.393
19	400	15000	120	2.108
20	400	15000	240	2.191
21	400	15000	360	2.253
22	400	22500	120	2.068
23	400	22500	240	2.263
24	400	22500	360	2.404
25	400	30000	120	2.115
26	400	30000	240	2.313
27	400	30000	360	2.315

### 3.6.2 Measurement of Cylindricity

The term "cylindricity" describes how closely something resembles a real cylinder. Cylindricity is a three-dimensional tolerance that assures a cylindrical feature's overall form is round and parallel to its axis. Any datum feature has no effect on cylinder symmetry, but the tolerance must be lower than the diameter dimensional tolerance of the component. In essence, cylindricity provides a perfect circular boundary around the item, inside which the entire three-dimensional section must fit.

Cylindricity was measured using Coordinate Measuring Machine. Coordinate Measuring Machine and its specifications are as depicted in figure 3.6 and table 3.6. The measurement of cylindricity and deviation is as shown in table 3.7



**Figure 3.6 Coordinate Measuring Machine**

**Table 3.6 Specifications of Coordinate Measuring Machine**

<b>Make</b>	ZEISS 3D CNC Co-Ordinate Measuring Machine (Contura G2)
<b>Accuracy</b>	1.8 $\mu$ m & 2.1 $\mu$ m.
<b>Measuring Range</b>	X = 700mm Y = 1000mm Z = 600mm
Fixed Probe Head for High Accuracy and Repeatability	

**Table 3.7 Measurement of Cylindricity**

Hole No.	Measured Value	Nominal Value	+ Tolerance	- Tolerance	Deviation	
1	0.0181	0.0000	0.1000	0.0000	0.0181	
2	0.0428	0.0000	0.1000	0.0000	0.0428	
3	0.0198	0.0000	0.1000	0.0000	0.0198	
4	0.0050	0.0000	0.1000	0.0000	0.0050	
5	0.0453	0.0000	0.1000	0.0000	0.0453	
6	0.0319	0.0000	0.1000	0.0000	0.0319	
7	0.0303	0.0000	0.1000	0.0000	0.0303	
8	0.0153	0.0000	0.1000	0.0000	0.0153	
9	0.0587	0.0000	0.1000	0.0000	0.0587	
10	0.0180	0.0000	0.1000	0.0000	0.0180	
11	0.0425	0.0000	0.1000	0.0000	0.0425	
12	0.0166	0.0000	0.1000	0.0000	0.0166	
13	0.0208	0.0000	0.1000	0.0000	0.0208	
14	0.0368	0.0000	0.1000	0.0000	0.0368	
15	0.0462	0.0000	0.1000	0.0000	0.0462	
16	0.0216	0.0000	0.1000	0.0000	0.0216	
17	0.0343	0.0000	0.1000	0.0000	0.0343	
18	0.0359	0.0000	0.1000	0.0000	0.0359	
19	0.0283	0.0000	0.1000	0.0000	0.0283	
20	0.0470	0.0000	0.1000	0.0000	0.0470	
21	0.0107	0.0000	0.1000	0.0000	0.0107	
22	0.0200	0.0000	0.1000	0.0000	0.0200	
23	0.0270	0.0000	0.1000	0.0000	0.0270	
24	0.0201	0.0000	0.1000	0.0000	0.0201	
25	0.0454	0.0000	0.1000	0.0000	0.0454	
26	0.0246	0.0000	0.1000	0.0000	0.0246	
27	0.0380	0.0000	0.1000	0.0000	0.0380	

The cylindricity tolerance zone is represented by two concentric cylinders, one on the inside and the other on the outside, that run the length of the drilled hole, forming a cylindrical boundary that is perfect across the full surface of the part.

The volume encompassed by the radial spacing between these two concentric cylinders is the cylindricity tolerance zone. The applicable cylindrical tolerance limitations are the difference in their diameters. As a result, the zone constrains the whole surface of the portion.

The axis of the cylindrical component corresponds with the common axis of the concentric cylinders in the tolerance zone. The positive (+) tolerance is set at 0.1000 mm, while the negative (-) tolerance is set at 0.0000 mm in this example.

The zone between these two concentric cylinders is approved for all places of the surface under supervision.

### 3.6.3 Measurement of Hole Depth

The hole depth is the distance from the surface of the workpiece up to which the hole is drilled. To measure the hole depth, the workpiece with drilled holes is cut across the cross section with the help of Wire Cut Electric Discharge Machine as the workpiece was found to be conductive from preliminary experiments. The wire cut EDM and its specifications are as shown in figure 3.7 and table 3.7.



**Figure 3.7 Wire Cut Electric Discharge Machine**

**Table 3.8 Specifications of Wire Cut Electric Discharge Machine**

<b>Make</b>	CONCORD Wire EDM – DK7732
<b>Table Travel X x Y</b>	320 x 400 mm
<b>Work Table Size L x W</b>	415 x 635 mm
<b>Max. Workpiece Thickness</b>	500 mm
<b>Max. Taper/100mm Thickness</b>	±3
<b>Max. Workpiece Weight</b>	400 kgs
<b>Machine Weight</b>	1800 kgs
<b>Maximum Speed</b>	400 mm <sup>2</sup> /min
<b>Machining Accuracy</b>	0.01 mm
<b>Surface Finish</b>	1.25 to 1.75 µm
<b>Thickness of Wire (Molybdenum)</b>	0.18 mm

The cross section of drilled holes is as shown in figure 3.8. The measurement of hole depth is done with the help of Vernier Height Gauge and the measurement is as shown in the figure 3.8. The values of hole depth are then measured and tabulated in Table 3.9.

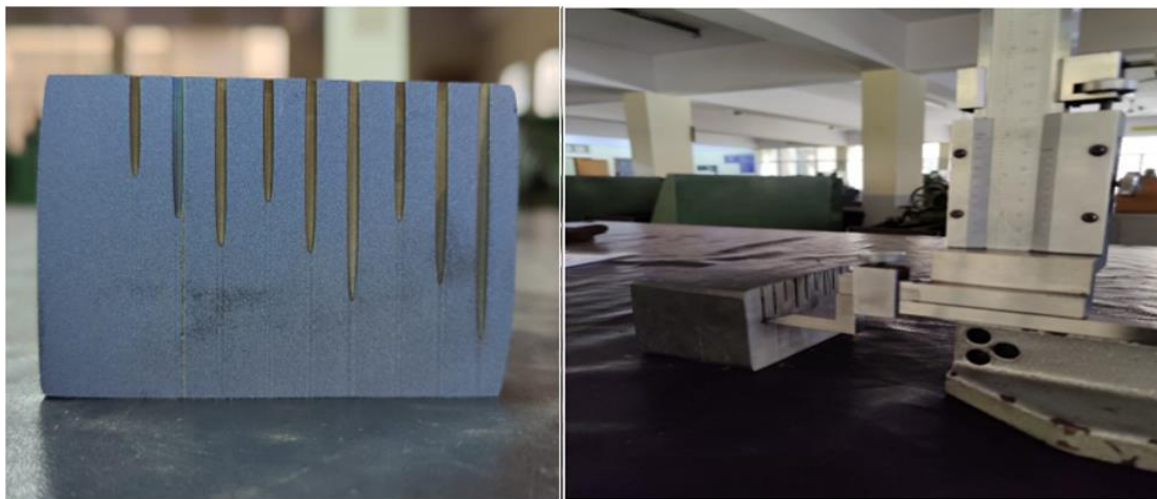


**Figure 3.8 Cross section of drilled holes & measurement using Vernier Height Gauge**

**Table 3.9 Values of Hole Depth**

<b>Sl. No.</b>	<b>Abrasive Flow Rate (g/min)</b>	<b>Water Pressure (psi)</b>	<b>Drilling Time (s)</b>	<b>Hole Depth (mm)</b>
<b>1</b>	200	15000	120	14.16
<b>2</b>	200	15000	240	21.20
<b>3</b>	200	15000	360	23.16
<b>4</b>	200	22500	120	16.58
<b>5</b>	200	22500	240	23.06
<b>6</b>	200	22500	360	30.08
<b>7</b>	200	30000	120	19.32
<b>8</b>	200	30000	240	26.76
<b>9</b>	200	30000	360	34.04
<b>10</b>	300	15000	120	15.02
<b>11</b>	300	15000	240	22.16
<b>12</b>	300	15000	360	26.84
<b>13</b>	300	22500	120	18.74
<b>14</b>	300	22500	240	25.90
<b>15</b>	300	22500	360	33.74
<b>16</b>	300	30000	120	21.36
<b>17</b>	300	30000	240	31.00
<b>18</b>	300	30000	360	38.50
<b>19</b>	400	15000	120	16.58
<b>20</b>	400	15000	240	23.38
<b>21</b>	400	15000	360	27.56
<b>22</b>	400	22500	120	20.18
<b>23</b>	400	22500	240	29.12
<b>24</b>	400	22500	360	36.38
<b>25</b>	400	30000	120	23.80
<b>26</b>	400	30000	240	33.38
<b>27</b>	400	30000	360	43.26

The hole created by AWJ drilling is much wider than the jet stream, owing to extra wall erosion caused by the powerful upward ejection of the jet out of the blind cavity. A very turbulent and chaotic flow state exists in the annular backflow zone surrounding the entering jet. The expelled stream is a churning combination of water and air, packed with broken and intact abrasive particles as well as removed material pieces. It interacts with the entering flow as well as the uneven, ever-changing hollow surface. The abrasive water jet is stopped after the drilling time reaches the desired value in each trial which leads to formation of a blind hole. Hence the end of the blind hole takes the shape of a cone.



## Chapter 4

# RESULTS AND DISCUSSION

ANOVA is used to determine the statistical significance of each input parameter, as well as the relative percentage contribution of each parameter to the output parameters and their interactions, as well as to estimate the error variance. A statistical model may be developed using this data to estimate the diameter and depth of the entrance hole. The statistical tables show that the parameter with an F-ratio more than the criterion is statistically significant, whereas the parameter with an F-ratio less than the criterion has no statistically significant influence on the output parameter. Similarly, the input parameter with a P-value lesser than the significance level influences the response parameter, whereas the parameter with a P-value larger than the significance level has no impact. [6]

The responses namely, entry hole diameter and hole depth were analysed using a general linear model with the help of ANOVA. The percentage contribution (% C), F-ratios, P-values of each input parameter to the overall variance are reported, demonstrating the degree of effect on entrance hole diameter and hole depth. The analysis was achieved at a confidence level of 95%, i.e., for a significance level of 0.05.

## 4.1 Entry Hole Diameter

In Table 4.1, the degree of influence on Entry Hole Diameter is shown by F-ratios, P-values, and the percentage contribution (% C) of each source to the overall variance.

**Table 4.1 ANOVA Table for entry hole diameter**

Source	DF	Seq SS	Contribution	Adj SS	Adj MS	F-Value	P-Value
Abrasive Flow Rate	2	0.092945	21.35%	0.092945	0.046472	22.01	0.001
Water Jet Pressure	2	0.054605	12.55%	0.054605	0.027302	12.93	0.003
Drilling Time	2	0.255177	58.63%	0.255177	0.127588	60.43	0.000
Abrasive Flow Rate * Water Jet Pressure	4	0.008131	1.87%	0.008131	0.002033	0.96	0.478
Abrasive Flow Rate * Drilling Time	4	0.004619	1.06%	0.004619	0.001155	0.55	0.707
Water Jet Pressure * Drilling Time	4	0.002885	0.66%	0.002885	0.000721	0.34	0.843
<b>Error</b>	8	0.016891	3.88%	0.016891	0.002111		
<b>Total</b>	26	0.043525	100.00%				



---

From the ANOVA table it can be observed that

- The F-ratios for AFR, WJP and DT in the preceding tables are higher than the F-ratios in the statistics tables. Furthermore, the P-values for these parameters derived from the ANOVA analysis are less than 0.05.
- As a result, it can be stated that these variables have the greatest statistical impact on the diameter of the entrance hole.
- Furthermore, because the interaction effects have P-values larger than 0.05, they are not significant.
- The contribution of AFR, WJP and DT on entry hole diameter was found to be 21.35 %, 12.55 %, 58.63 % respectively.
- The total contribution of AFR, WJP and DT amounts to around 92.5% on entry hole diameter.
- Percentage contribution of interactions, that is, AFR & WJP, AFR & DT and WJP & DT adds up to around 3.6%, but the interaction effects are not significant and hence can be neglected.
- The percentage error column around 3.8 percent reflects the impact of other parameters on the entrance hole diameter, such as orifice and focusing nozzle diameters, abrasive size fluctuation in the waterjet, and so on.
- The interaction of AFR, WJP and DT is not considered in ANOVA.

The main effect plots for entry hole diameter is as shown in figure 4.1. The following inferences can be made from the graph:

- As the AFR increased, the entry hole diameter increases. As the AFR rises, the divergence of abrasive particles increases, resulting in a larger entry hole diameter.
- The entry hole diameter grows as the WJP and DT increase. The divergence of the abrasive water jet grows as the WJP and DT increase, resulting in an increase in entry hole diameter.

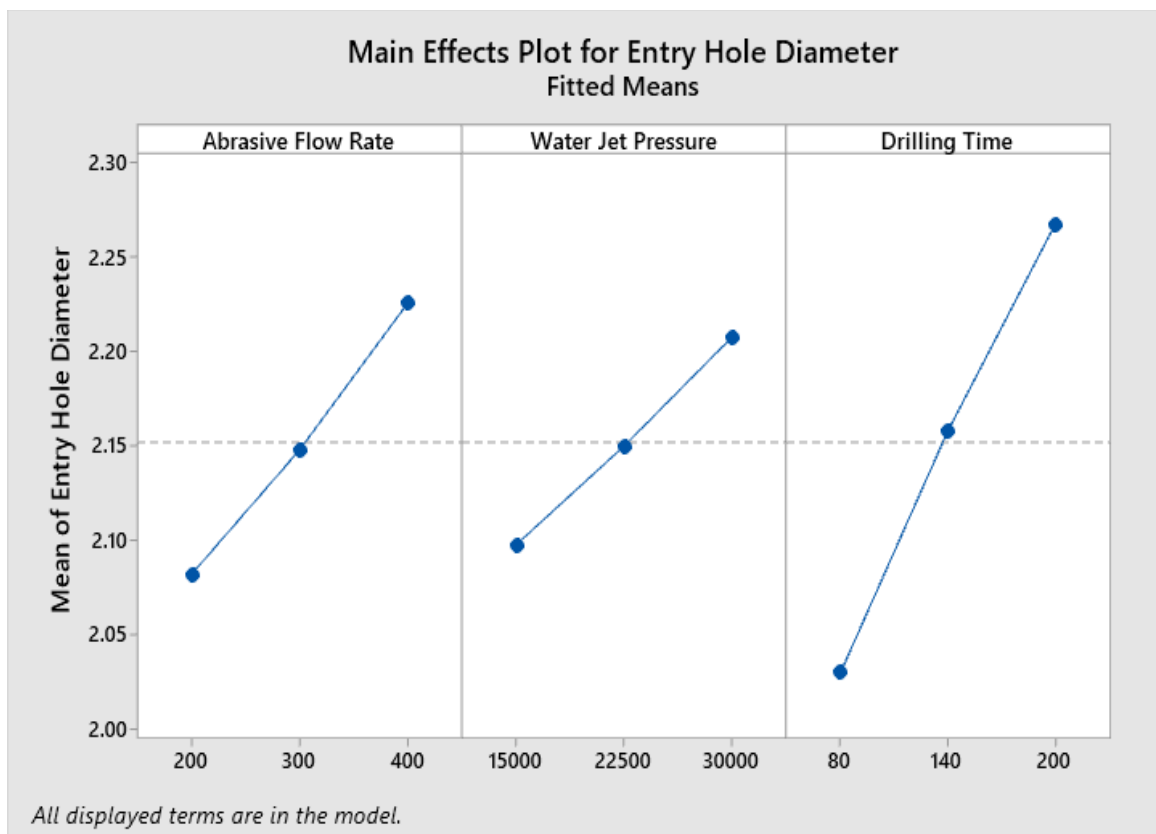


**Figure 4.1 Main Effects Plot for Entry Hole Diameter**

The regression equation is used to determine whether or not the input and output parameters are related. It's an algebraic equation that predicts the dependent variable's value based on the independent variables' values. It was obtained with the help of Minitab statistical software. In the regression equation, statistically significant variables are incorporated.

The regression equation for entry hole diameter is as follows:

$$\text{Entry Hole Diameter} = a + b(\dot{m}) + c(P) + d(t) + \varepsilon \quad 4.1$$

where,

Constant,  $a = 1.52$

Regression Coefficients,  $b = 0.000718$

$$c = 0.000007$$

$$d = 0.001982$$

$\varepsilon$  = Error

$\dot{m}$  is Abrasive Flow Rate,  $P$  is Water Jet Pressure,  $t$  is Drilling Time

The diameter of the entrance hole, which was measured using a profile projector, was compared to the values obtained using the regression equation. The comparison between the two values and the percentage error is calculated and is as shown in the table 4.2. The percentage error is calculated using the formula

$$\text{Percentage error} = \frac{\text{Experimental Value} - \text{Calculated Value}}{\text{Experimental Value}} \times 100 \quad 4.2$$

As the analysis was done at 95 % confidence level and there were other factors affecting the entry hole diameter such as dimensions of orifice and focusing nozzle, variation in size of abrasives used in the waterjet, the errors obtained is in the acceptable limit. Hence, the obtained regression equation is deemed as fit and can be used to predict the values of entry hole diameter for different values of Abrasive Flow Rate, Water Jet Pressure, Drilling Time other than the experimental values.

**Table 4.2 Error Analysis of regression equation for Entry Hole Diameter**

Hole No.	Experimental Value	Calculated Value	Percentage Error
1	1.909	1.927	0.94
2	2.024	2.046	1.08
3	2.136	2.165	1.34
4	1.957	1.980	1.14
5	2.078	2.099	0.98
6	2.184	2.218	1.51
7	2.044	2.032	0.58
8	2.124	2.151	1.26
9	2.282	2.270	0.53
10	1.942	1.999	2.85
11	2.125	2.118	0.34
12	2.191	2.237	2.05
13	2.035	2.051	0.80
14	2.110	2.170	2.78
15	2.251	2.289	1.67
16	2.090	2.104	0.66
17	2.194	2.223	1.30
18	2.393	2.342	2.19
19	2.108	2.071	1.80
20	2.191	2.190	0.06
21	2.253	2.309	2.41
22	2.068	2.123	2.60
23	2.263	2.242	0.93
24	2.404	2.361	1.82
25	2.115	2.176	2.79
26	2.313	2.295	0.80
27	2.315	2.414	4.09

## 4.2 Hole Depth

In Table 4.3, the degree of influence on Hole Depth is shown by F-ratios, P-values, and the percentage contribution (% C) of each source to the overall variance.

**Table 4.3 ANOVA Table for Hole Depth**

Source	DF	Seq SS	Contribution	Adj SS	Adj MS	F-Value	P-Value
Abrasive Flow Rate	2	114.28	7.87%	114.28	57.141	129.33	0.000
Water Jet Pressure	2	368.43	25.38%	368.43	184.216	416.93	0.000
Drilling Time	2	910.61	62.74%	910.61	455.307	1030.49	0.000
Abrasive Flow Rate * Water Jet Pressure	4	10.89	0.75%	10.89	2.722	6.16	0.015
Abrasive Flow Rate * Drilling Time	4	7.87	0.54%	7.87	1.968	4.45	0.035
Water Jet Pressure * Drilling Time	4	35.87	2.47%	35.87	8.967	20.29	0.000
<b>Error</b>	8	3.53	0.24%	3.53	0.442		
<b>Total</b>	26	1451.49	100.00%				

From the ANOVA table it can be observed that

- The contribution of abrasive flow rate ( $\alpha$ ), water jet pressure ( $\beta$ ) and drilling time ( $\gamma$ ) on hole depth was found to be 7.87 %, 25.38 %, 62.74 % respectively.
- The total contribution of AFR, WJP and DT amounts to around 96% on hole depth.
- Percentage contribution of interactions, that is, AFR & WJP, AFR & DT and WJP & DT adds up to around 3.7%, and the interaction effects are significant and is to be included in the regression equation.
- The percentage error column around 0.24 % reflects the impact of other parameters on the entrance hole diameter, such as orifice and focusing nozzle diameters, abrasive size fluctuation in the waterjet, and so on
- The interaction of abrasive flow rate, waterjet pressure and drilling time ( $\alpha\beta\gamma$ ) is not considered in ANOVA.

The regression equation is an algebraic equation which determines the relationship between the input parameters and the output parameters. For hole depth, it was found that mass flow rate, WJP and DT was found to be statistically significant and was to be included in the regression equation. The interactions between the input parameters, that is, AFR & WJP ( $\alpha$  &  $\beta$ ), AFR & DT ( $\alpha$  &  $\gamma$ ), WJP & DT ( $\beta$  &  $\gamma$ ) were also found to be significant and hence they were also included. Since the interactions were found to be significant, they were included in the regression equation. As the individual terms and the interactions were to be

included in the regression equation, a quadratic equation involving both the individual and the interaction terms was formulated. The regression equation along with the regression coefficients was obtained with the use of Minitab software. The regression equation for hole depth is as follows:

$$\text{Hole Depth} = a + b(\dot{m}) + c(P) + d(t) + e(\dot{m}^2) + f(P^2) + g(t^2) + h(\dot{m}P) + i(\dot{m}t) + j(Pt) \quad 4.3$$

The regression coefficients are

a	b	c	d	e	f	g	h	i	j
5.19	0.0064	0.000011	0.0523	0.000025	0.000001	0.000195	0.000001	0.000131	0.000004

$\dot{m}$  is Abrasive Flow Rate,  $P$  is Water Jet Pressure,  $t$  is Drilling Time

The main effect plots for hole depth is as shown in figure 4.2. The following inferences can be made from the graph.

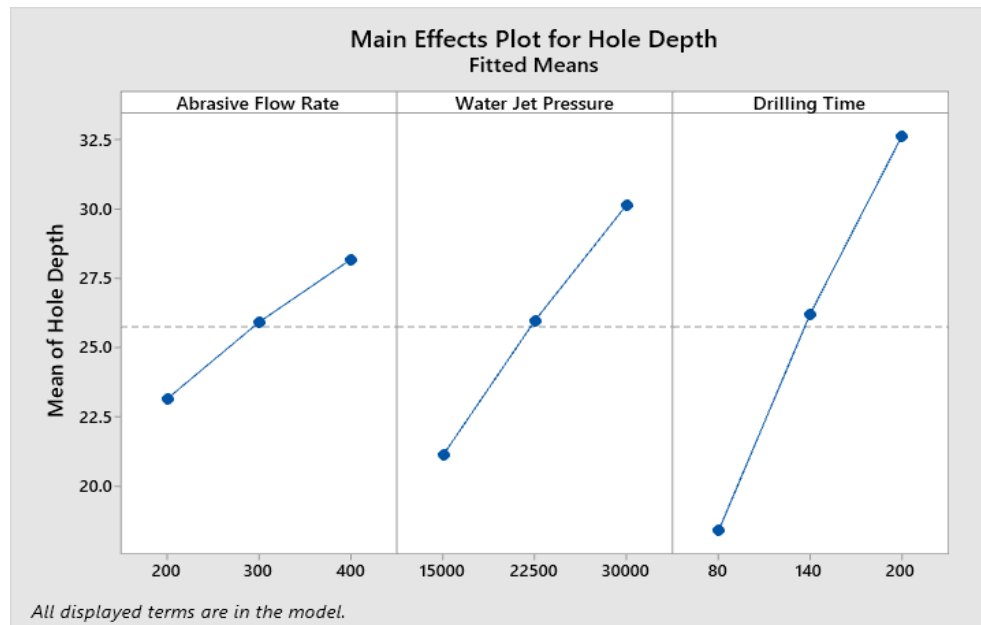


**Figure 4.2 Main Effects Plot for Hole Depth**

- As the AFR increased, the hole depth is increased. This is because when the AFR increases, a higher number of abrasive particles engage in eroding the target material.
- As the WJP is increased, the hole depth is increased. Because the velocity of abrasive particles is quite fast, the energy held by the jet increases as the WJP increases.
- The hole depth is observed to grow as DT is increased. This is owing to the fact that when DT rises, abrasive particles involved in erosion are in touch with the target material for longer periods of time.

The values of hole depth which was measured with the help of vernier height gauge and was compared with the values calculated with the help of the regression equation. The comparison between the two values and the percentage error is calculated and is as shown in the table 4.4. The percentage error is calculated using equation 4.2. As the analysis was done at 95 % confidence level and there were other factors affecting the hole depth such as dimensions of orifice and focusing nozzle, variation in size of abrasives used in the waterjet, the errors obtained is in the acceptable limit. Hence, the obtained regression equation is deemed as fit and can be used to predict the values of hole depth for different values of Abrasive Flow Rate, Water Jet Pressure, Drilling Time other than the experimental values.

**Table 4.4 Error Analysis of regression equation for Hole Depth**

Hole No.	Experimental Value	Calculated Value	Percentage Error
1	14.16	14.26	0.70
2	21.20	20.94	1.24
3	23.16	22.54	2.75
4	16.58	16.60	0.12
5	23.06	22.46	2.67
6	30.08	29.88	0.67
7	19.32	19.42	0.51
8	26.76	26.84	0.30
9	34.04	33.92	0.35
10	15.02	15.08	0.40
11	22.16	22.42	1.16
12	26.84	27.01	0.63
13	18.74	17.96	4.34
14	25.90	26.22	1.22
15	33.74	32.64	3.37
16	21.36	22.08	3.26
17	31.00	30.96	0.13
18	38.50	38.30	0.52
19	16.58	16.22	2.22
20	23.38	23.12	1.12
21	27.56	27.24	1.17
22	20.18	21.02	4.00
23	29.12	28.96	0.55
24	36.38	35.91	1.31
25	23.80	23.64	0.68
26	33.38	32.88	1.52
27	43.26	44.04	1.77

### 4.3 Scanning Electron Microscopy/ EDX Analysis

The SEM images are used in the characterization of abrasive water jet drilled holes. Since there are 27 holes and all the holes cannot be taken into account during the characterization, scanning electron microscope images of three holes, that is, hole with minimum hole depth, hole with intermediate hole depth, hole with maximum hole depth are considered for analysis.

#### 4.3.1 SEM and EDX analysis of hole with minimum hole depth

The SEM images of hole drilled with AFR at 200 g/min, WJP at 15000 psi, DT at 120 seconds is as shown in figure 4.3. The observations from the SEM images is recorded in section 4.3.3.

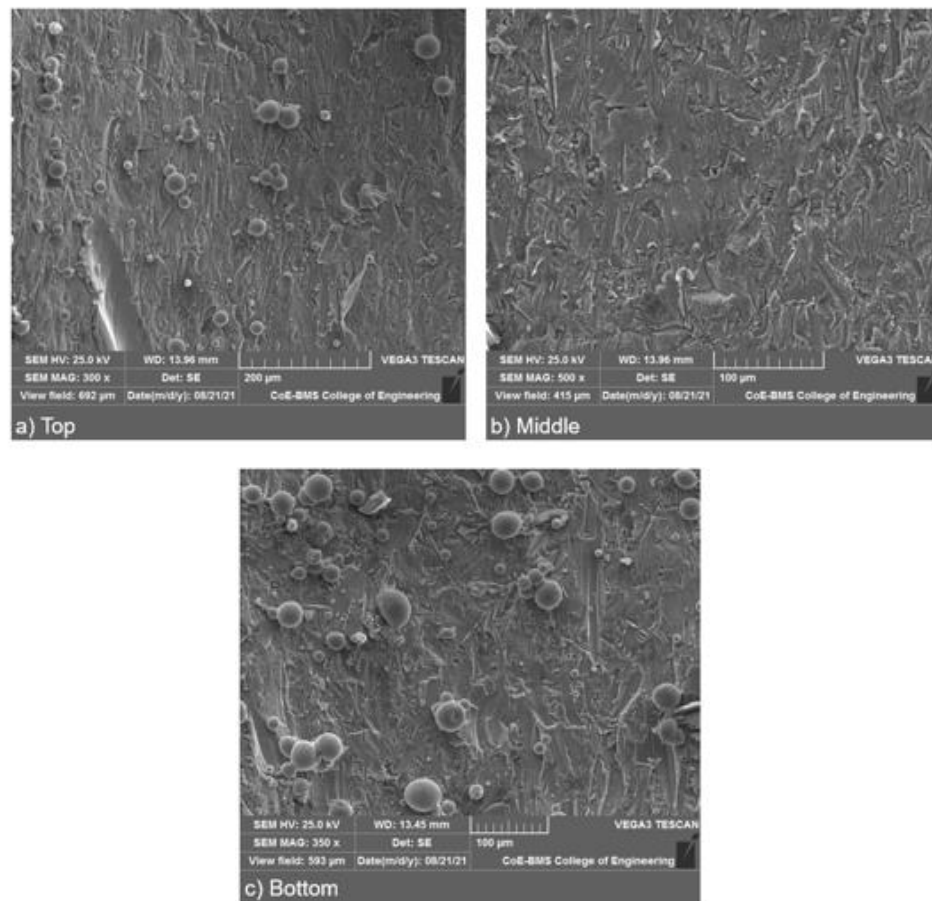


**Figure 4.3 SEM images of hole drilled with AFR at 200 g/min, WJP at 15000 psi & DT at 120 seconds (Minimum Hole Depth)**

The X-ray technique Energy Dispersive X-Ray Analysis (EDX), often known as EDS or EDAX, is used to determine the elemental composition of materials. EDX analysis produces spectra with peaks corresponding to the elements that make up the real

composition of the material under investigation. The use of EDX was used to determine the chemical composition of the workpiece.

Figure 4.4 and table 4.5 shows the results of EDX analysis and the observations from EDX analysis is recorded in section 4.3.3.

### EDX Analysis

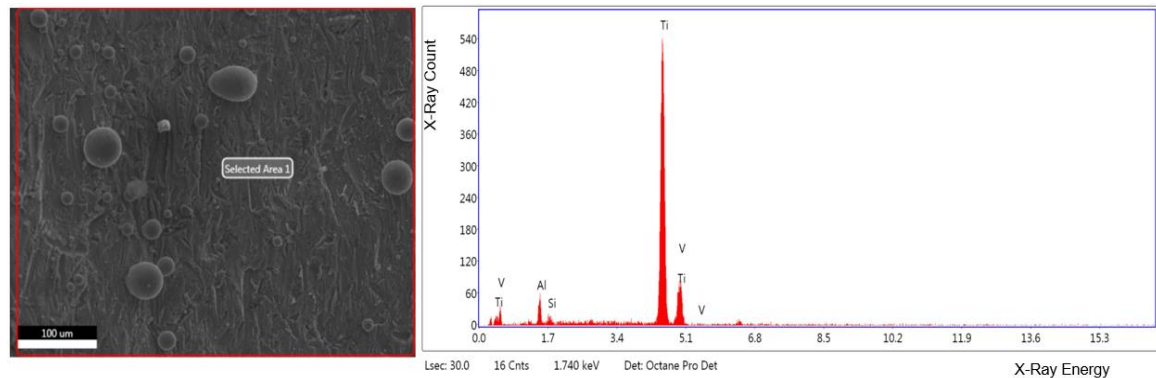


**Figure 4.4 EDX spectrum of hole with minimum hole depth**

**Table 4.5 EDX analysis results of hole with minimum hole depth**

Element	Shell	Weight %
Al	K	5.52
Si	K	1.42
Ti	K	88.16
V	K	4.90

### 4.3.2 SEM analysis of hole with intermediate hole depth

The SEM images of hole drilled with AFR at 300 g/min, WJP at 15000 psi, DT at 240 seconds is as shown in figure 4.5. The observations from the SEM images is recorded in section 4.3.3.



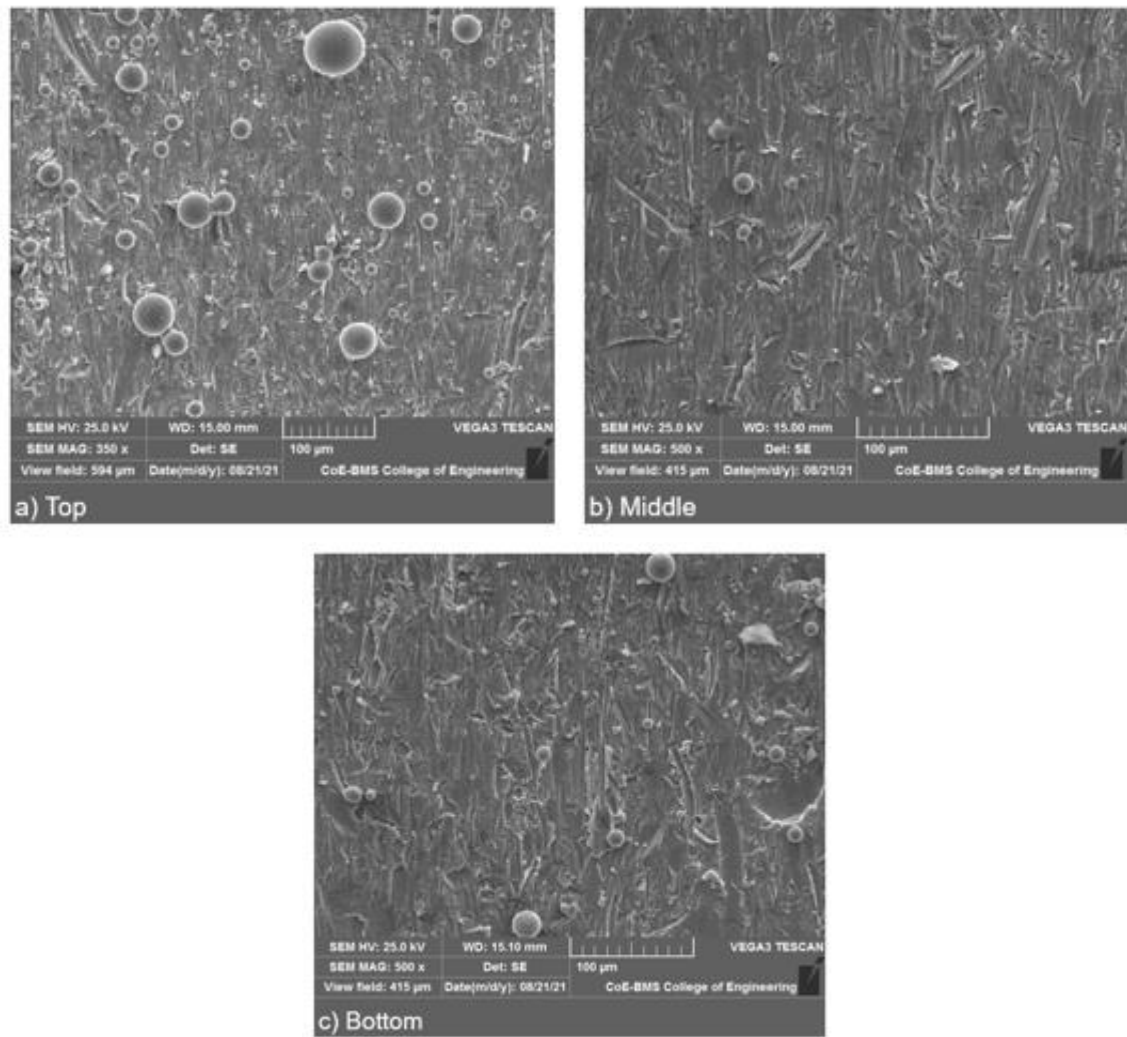


**Figure 4.5 SEM images of hole drilled with AFR at 300 g/min, WJP at 15000 psi, DT at 240 seconds (Intermediate Hole Depth)**

#### **4.3.3 SEM and EDX analysis of hole with maximum hole depth**

The SEM images of hole drilled with AFR at 400 g/min, WJP at 30000 psi, DT at 360 seconds is as shown in figure 4.6. The observations from the SEM images is recorded in section 4.3.3.

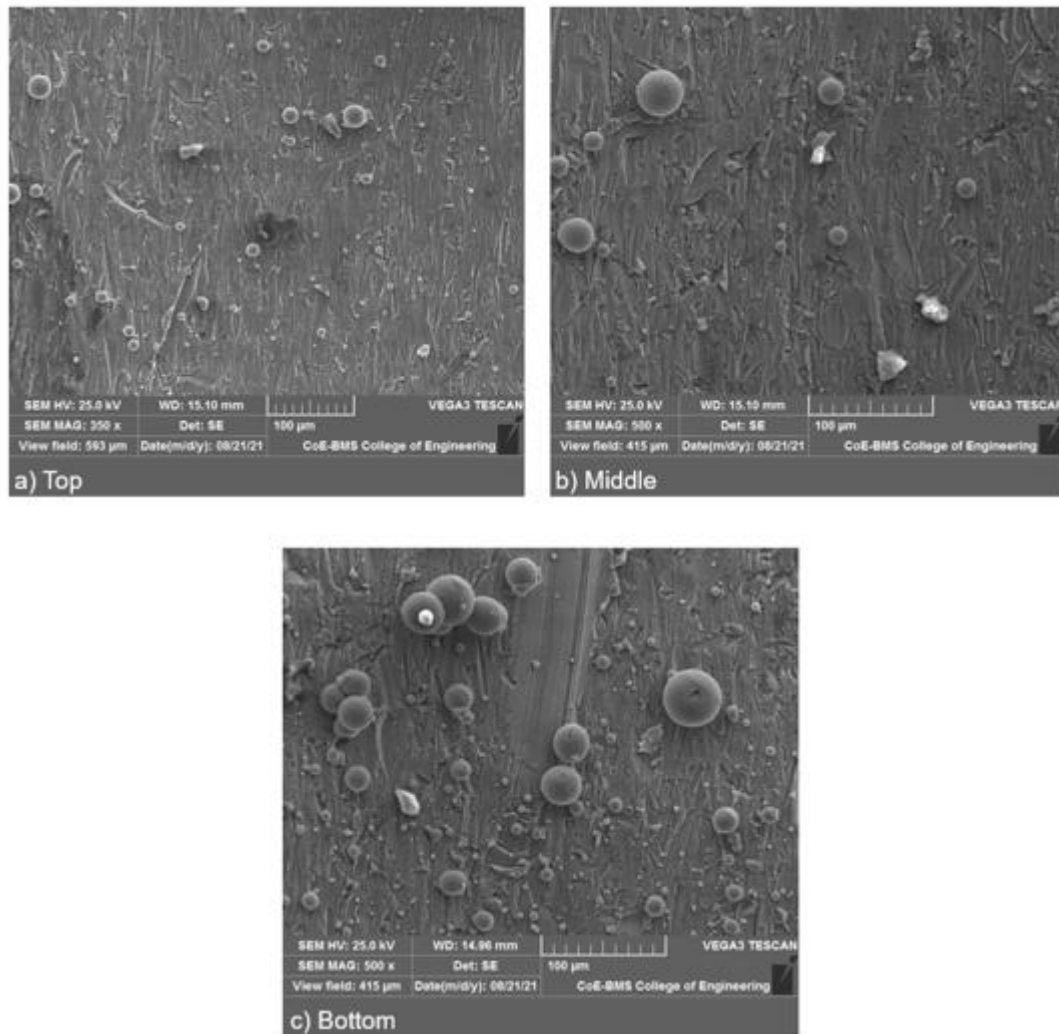


**Figure 4.6 SEM images of hole drilled with Abrasive flow rate at 400 g/min, Water jet pressure at 30000 psi, drilling time at 360 seconds (Maximum Hole Depth)**

In order to find out the chemical composition of the workpiece, EDX was utilized which gives the distribution and concentration of the elements in the sample. the observations from EDX analysis is recorded in section 4.3.3.

### EDX Analysis

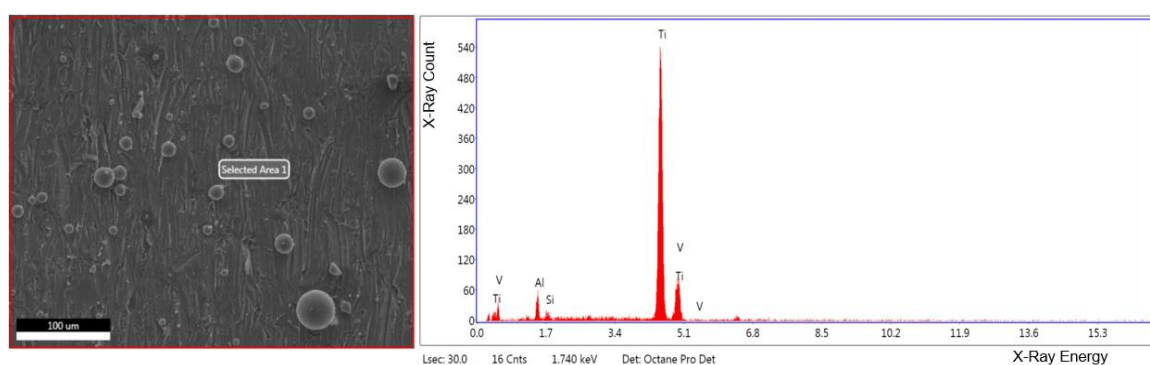


**Figure 4.7 EDX spectrum of hole with maximum hole depth**

**Table 4.6 EDX analysis results of hole with maximum hole depth**

Element	Shell	Weight %
Al	K	5.38
Si	K	1.06
Ti	K	88.15
V	K	5.41

#### 4.3.4 Observations from SEM and EDX analysis

The SEM images of three different drilled holes are as shown in the figure 4.3, 4.5 and 4.6.

The observations from the SEM and EDX analysis are as follows:

- From figure 4.3 (a), 4.3 (b), 4.3 (c) it was seen that the eroded surface was very rough and the eroded particles are not in uniform in their shape and size.
- The metal substrate was analysed using EDX Analysis to determine the weight percentage of each element and was found that Titanium, Aluminium and Vanadium had higher weight percentages as seen in table 8. This is due to the fact that when material is removed by abrasive water jet, due to raise in localized temperatures in some areas, the eroded particles are adhered to the substrate.
- The Silica element found in the EDX analysis is found to have the weight percentage of around 1.06%. This is because 98.5% of the abrasive particles entrained in the water jet participate in the material removal and that energy is harnessed to cut the material. About 1.5% do not participate in the erosion mechanism and are lodged on the surface as their kinetic energy is less to cut the material. This residue is reflected in the EDX analysis.
- The SEM images and EDX analysis of the intermediate hole depth and maximum hole depth are as shown in figure 4.5 (a), 4.5 (b), 4.5 (c) & 4.6 (a), 4.6 (b), 4.6 (c) and table 4.6 respectively. The same trend was seen in the SEM images of intermediate hole depth and maximum hole depth.

---

## Chapter 5

# CONCLUSION

Abrasive Water Jet Drilling, a non-traditional machining technique was used to drill Ti6Al4V and was performed based on the experiments designed according to Taguchi method. The conclusions that can be drawn from analysis of the hole profile are as follows:

- Entry Hole Diameter was found to increase with increase in input parameters, that is, abrasive flow rate, water jet pressure, drilling time based on ANOVA results. It was not significantly affected by the interactions between the input parameters and hence was neglected in the formulation of regression equation.
- Cylindricity was measured for all the 27 holes and it was found that all the holes were within the tolerance limit of 0.1 mm. If the tolerance limit is within 0.025 mm, the deviations obtained in this study does not adhere to it. Hence, for accurately drilling of hole with tolerance limit less than 0.025 mm, abrasive water jet drilling cannot be used for this material.
- Hole depth was found to increase with increase in input parameters, that is, abrasive flow rate, water jet pressure, drilling time based on ANOVA results. It was significantly affected by the interactions between the input parameters and hence was included in the formulation of regression equation.
- The SEM images of three different drilled holes are as shown in the images above and the eroded surface is found to be very rough and the eroded particles are not in uniform in their shape and size and when analysed using Energy Dispersive X-Ray Analysis it was found that Titanium, Aluminium and Vanadium had higher weight percentages. This is due to the fact that when material is removed by abrasive water jet, due to raise in localized temperatures in some areas, the eroded particles are adhered to the substrate. The silica elements found during EDX analysis is due to the residue of abrasive particles.
- This research work can be used as a data bank in machining industries for applications such as marine industries where drilling of Ti6Al4V is necessary.

- There is scope for further study where these experimental results can be validated using Finite Element Analysis.
- It may also be used as a starting point for a research to construct an empirical and analytical model to determine the link between input and output characteristics such as entry hole diameter and hole depth.

---

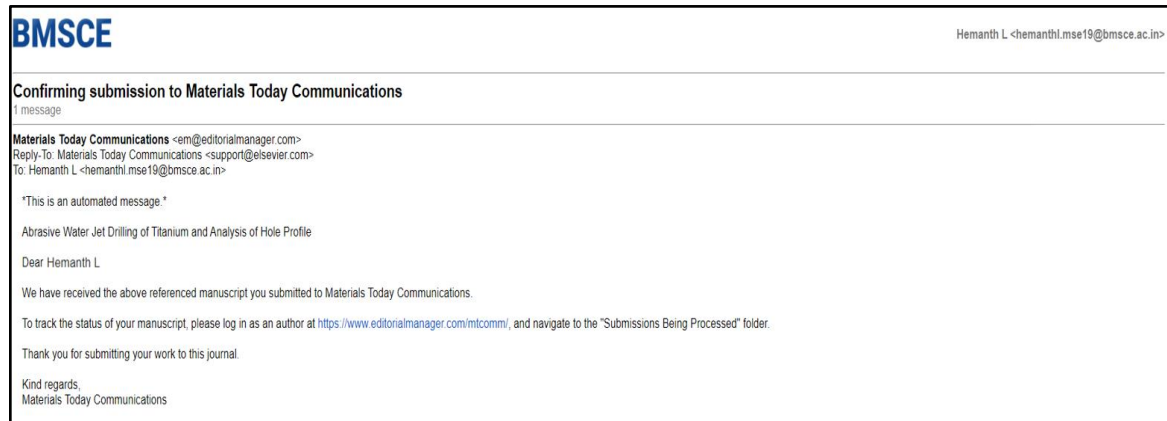
## REFERENCES

- [1] [https://irjiet.com/common\\_src/article\\_file/1574433481\\_74ed6f218b\\_3\\_irjiet.pdf](https://irjiet.com/common_src/article_file/1574433481_74ed6f218b_3_irjiet.pdf)
- [2] <https://www.azom.com/article.aspx?ArticleID=1547>
- [3] Li, H., Wang, J. An experimental study of abrasive waterjet machining of Ti-6Al-4V. *Int J Adv Manuf Technol* 81, 361–369 (2015).
- [4] Jegaraj JJR, Babu NR, 2007, “A soft computing approach for controlling the quality of cut with abrasive water jet cutting system experiencing orifice and focusing to wear”, *J Mater Process Technol*, 185, pp. 217-227.
- [5] LiW, Wang J, Zhu H, Huang C (2013) On ultrahigh velocity micro-particle impact on titanium—a single impact study. *Wear* 35(1–2):216–227.
- [6] Caydas U, Hascalik A, 2008, “A study on surface roughness in abrasive water jet machining process using Titanium Alloy and regression analysis method”, *J Mater Process Technol*, 202, pp. 574-582.
- [7] S.M. Afazova, R. Ronaldo, D. Lonsdale, D. Zdebski, S.M. Ratchev, “Analysis of micro-drilling of glassy ceramic Macor nozzles for scanning droplet systems”, *Journal of Materials Processing Technology* 213 (2013) 221–228.
- [8] Alberdi A, Artaza T, Suarez A, Rivero A, Girot F. An experimental study on abrasive waterjet cutting of CFRP/Ti6Al4V stacks for drilling operations. *Int J Adv Manuf Technol* 2016;86(1-4):691–704.
- [9] Escobar-Palafox GA, Gault R, Ridgway K. Characterisation of abrasive water-jet process for drilling titanium and carbon fibre reinforced polymer stacks. *Surfaces* 2012;13:14.
- [10] Chang CW, Kuo CP, 2007, “Evaluation of surface roughness in laser-assisted machining of Titanium oxide ceramics with Taguchi method”, *Int J Mach Tool Manuf*, 47, pp. 141-147.

---

## PUBLICATION DETAILS

Hemanth L, Srinivas S, “Abrasive Water Jet Drilling of Titanium and analysis of Hole Profile”, *Materials Today Communications* (Submitted).



---

## Abrasive Water Jet Drilling of Titanium and Analysis of Hole Profile

Hemanth L<sup>1, a \*</sup>, Srinivas S<sup>2, b</sup>

<sup>1</sup> M. Tech Student, Department of Mechanical Engineering, B.M.S. College of Engineering, Bengaluru, India

<sup>2</sup> Professor, Department of Mechanical Engineering, B.M.S. College of Engineering, Bengaluru, India

<sup>a</sup>hemanthl.mse19@bmsce.ac.in, <sup>b</sup>drss.mech@bmsce.ac.in

**Keywords:** Abrasive Water Jet Drilling, Titanium Alloy, Cylindricity, ANOVA

**Abstract:** Ti6Al4V is an alpha-beta Titanium alloy with high specific strength and excellent corrosion resistance. These cannot be machined using traditional machining methods because of their poor machinability and low thermal conductivity. This work is focused on the analysis of profile of the holes drilled in Ti6Al4V by abrasive water jet drilling to understand the effect of cutting parameters such as abrasive flow rate, water jet pressure and drilling time. ANOVA was carried out to determine the most influential parameters. It was found that abrasive flow rate, water jet pressure, drilling time are statistically significant and their interaction effects, that is, abrasive flow rate & water jet pressure, abrasive flow rate & drilling time and water jet pressure & drilling time were not statistically significant in variation of entry hole diameter and abrasive flow rate, water jet pressure, drilling time and the interaction effects, that is, abrasive flow rate & water jet pressure, abrasive flow rate & drilling time and water jet pressure & drilling time were found to be statistically significant in variation of hole depth.

### 1. Introduction:

Titanium alloys have significant applications in aerospace, power generation and biomedical industries. It has excellent strength-to-weight ratio, high fracture resistance characteristics and exceptional corrosion resistance. Ti-6Al4V is the most commonly used titanium alloy and this alpha-beta alloy is regarded as the workhorse of the titanium industry. However, titanium alloys are difficult to machine by traditional mechanical methods because of their poor machinability. Nontraditional machining methods such as abrasive waterjet (AWJ) machining have been applied to overcome these problems [1]. Abrasive waterjet (AWJ) machining is a non-traditional machining process that employs high-pressure water for producing high velocity stream, entrained with abrasive particles



for cutting a wide variety of materials ranging from soft to hard materials. It is a versatile process since AWJs can be employed for many manufacturing applications such as cutting, milling, cleaning and surface treatment. AWJ cutting offers certain unique benefits such as negligible heat affected zone, high degree of maneuverability in cutting process and less machining force exertion. However, it is a complex process since the mechanism of material removal depends on the level of various process parameters and is explained by multiple phenomena and waviness observed in the deformation zone is the major drawback. AWJ cutting process parameters can be categorized into hydraulic, abrasive, mixing and cutting parameters [2]. J. John et al. explored the machinability of AWJ of 6063-T6-Aluminium alloy with abrasive flow rate, orifice size, focusing tube size, water jet pressure, traverse rate as input parameters and depth of cut, kerf width & surface roughness as output parameters based on Taguchi method of design of experiments. ANOVA was used to analyze the performance of AWJs in cutting and build empirical models and was conformed experimentally [1]. Weiyi Li et al. studied the AWJ machining of AISI 4340 Steel with the help of FE model and its conformity with the experimental data [3]. Ulas Caydas et al. investigated the machinability of 7075 Aluminium alloy by AWJ with Traverse Speed, Water Jet Pressure, Standoff Distance, Abrasive Grit Size, Abrasive Flow Rate as input parameters and surface roughness as output parameters. The design of experiments was based on Taguchi's method. Analysis of Variance was done to determine the significant factors and SEM investigations were also done [4]. Several other research works was based on AWJ machining of materials such as Macor (Machinable Glass Ceramic) [5], CFRP/Ti6Al4V stacks [6,7]. ANOVA and regression analysis were extensively used by researchers in determining the relationship between the input parameters and the output parameters. From the literature review, it can be observed that work was carried out in the field of abrasive water jet machining of different titanium alloys and other metals with different cutting parameters. But, limited work has been carried in the field of non-traditional drilling of Ti6Al4V. Hole drilling of Ti6Al4V is an important and challenging task for the manufacturing industry. In this work, drilling of holes with abrasive flow rate, water jet pressure, drilling time as the input parameters was carried out. The measured responses are entry hole diameter, hole depth, cylindricity. SEM images of the drilled profile were also studied in this work. Analysis of variance of the output parameters is used to identify the pattern in which process parameters affects the performance of the process and determine the significant parameters.

## 2. Materials and Methodology:

### 2.1 Materials used:

The material used in this work is Ti6Al4V which is a Titanium alloy. The chemical composition of the alloy is given in Table 1.

**Table 1 Chemical Composition of Ti6Al4V [2]**

Element	V	Al	Sn	Zr	Mo	C	Si	Cr	Ni	Fe	Cu	Nb	Ti
Weight %	4.22	5.48	0.06	0.002	0.005	0.36	0.02	0.009	0.001	0.112	0.02	0.03	90

### 2.2 Experimental Procedure:

The experimentation was carried out using the OMAX Corporation (MAXIEM 1515) AWJ Machine with 5 axes machining up to 59° taper and 8000 mm/min traverse speed. Preliminary experiments were carried out to design the experiments and assess the values and levels of the process parameters. A complete factorial design ( $3^3$ ) based on Taguchi Method was implemented to study the effects of Abrasive Flow Rate (AFR), Water Jet Pressure (WJP), Drilling Time (DT) on the entry hole diameter, hole depth, cylindricity of the holes drilled with the help of AWJM. The process parameters for AWJ drilling is as shown in Table 2 and the setup of the AWJ of Titanium alloy is as shown in figure 1. The other parameters such as stand-off distance, abrasive mesh size and material, orifice diameter, impact angle were kept constant.

**Table 2 Process parameters for Abrasive Water Jet Drilling**

Factors	Level 1	Level 2	Level 3
Water Pressure (psi)	15000	22500	30000
Abrasive Flow Rate (g/min)	200	300	400
Drilling Time (s)	80	140	200
Standoff Distance (mm)	3		
Abrasive Mesh size	80		
Orifice Diameter (mm)	0.25		
Focusing nozzle diameter (mm)	1.07 and material is Tungsten Carbide		
Abrasive Material	Garnet		
Impact Angle	90°		



**Figure 1 Setup of Abrasive Water Jet Drilling of Ti6Al4V**

### **3. Results and Discussion:**

The quality of the holes drilled using Abrasive Water Jet Drilling Process were evaluated with the help of Profile Projector, Coordinate Measuring Machine, Vernier Height Gauge and Scanning Electron Microscope.

#### **3.1 Measurement of Entry Hole Diameter**

To measure the entry hole diameter a Nikon V24B profile projector which has a magnification accuracy of 0.05% for contour illuminations and 0.075% for surface illuminations, effective screen diameter of 600 mm was used. The entry hole diameter was measured using the profile projector and was tabulated and is as shown in Table 3. ANOVA was performed to determine the significant factors among AFR, WJP, DT and a regression equation was modelled to predict the effect of process parameters on entry hole diameter. ANOVA was done with the help of Minitab software. The ANOVA table for entry hole diameter is as shown in Table 4. The observations from the ANOVA table are as follows:

The F-ratios presented in table 4 for Abrasive Flow Rate, Water Jet Pressure and Drilling Time are more than F-ratios given in the statistical tables. Further, the P-values obtained from the ANOVA analysis for these parameters are less than 0.05. Therefore, it can be concluded that these parameters are most statistically significant parameters influencing the entry hole diameter. Further, the interaction effects are not significant as their P-values

---

are greater than 0.05. The contribution of abrasive flow rate, water jet pressure and drilling time on entry hole diameter was found to be 21.35 %, 12.55 %, 58.63 % respectively. The total contribution of abrasive flow rate, waterjet pressure and drilling time amounts to around 92.5 % on entry hole diameter. Percentage contribution of interactions, that is, abrasive flow rate and waterjet pressure, abrasive flow rate and drilling time, waterjet pressure and drilling time adds up to around 3.6%, but the interaction effects are not significant and hence can be neglected.

The percentage error column around 3.8 % indicates the contribution of other parameters such as dimensions of orifice and focusing nozzle, variation in size of abrasives used in the waterjet and etc. on the entry hole diameter. The interaction of abrasive flow rate, waterjet pressure and drilling time is not considered in ANOVA. The main effect plots for entry hole diameter is as shown in figure 2. The following inferences can be made from the graph:

The entry hole diameter was found to increase with increase in abrasive flow rate. As the abrasive flow rate increases there is an increase in scattering of abrasive particles that leads to increase in entry hole diameter. It was observed that entry hole diameter increases with increase in water jet pressure and drilling time. When there is a rise in in water jet pressure and drilling time, the divergence of the abrasive water jet increases and as a result there is an increase in entry hole diameter.

**Table 3 Values of Entry Hole Diameter, Hole Depth, Cylindricity Deviation**

Sl. No.	Abrasive Flow Rate (g/min)	Water Pressure (psi)	Drilling Time (s)	Entry Hole Diameter (mm)	Hole Depth (mm)	Cylindricity Deviation (mm)
1	200	15000	80	1.909	14.16	0.0181
2	200	15000	140	2.024	21.20	0.0428
3	200	15000	200	2.136	23.16	0.0198
4	200	22500	80	1.957	16.58	0.0050
5	200	22500	140	2.078	23.06	0.0453
6	200	22500	200	2.184	30.08	0.0319
7	200	30000	80	2.044	19.32	0.0303
8	200	30000	140	2.124	26.76	0.0153
9	200	30000	200	2.282	34.04	0.0587
10	300	15000	80	1.942	15.02	0.0180
11	300	15000	140	2.125	22.16	0.0425
12	300	15000	200	2.191	26.84	0.0166
13	300	22500	80	2.035	18.74	0.0208
14	300	22500	140	2.110	25.90	0.0368
15	300	22500	200	2.251	33.74	0.0462
16	300	30000	80	2.090	21.36	0.0216
17	300	30000	140	2.194	31.00	0.0343
18	300	30000	200	2.393	38.50	0.0359
19	400	15000	80	2.108	16.58	0.0283
20	400	15000	140	2.191	23.38	0.0470
21	400	15000	200	2.253	27.56	0.0107
22	400	22500	80	2.068	20.18	0.0200
23	400	22500	140	2.263	29.12	0.0270
24	400	22500	200	2.404	36.38	0.0201
25	400	30000	80	2.115	23.80	0.0454
26	400	30000	140	2.313	33.38	0.0246
27	400	30000	200	2.315	43.26	0.0380

**Table 4 ANOVA Table for entry hole diameter**

Source	DF	Seq SS	Contribution	Adj SS	Adj MS	F-Value	P-Value
Abrasive Flow Rate	2	0.092945	21.35%	0.092945	0.046472	22.01	0.001
Water Jet Pressure	2	0.054605	12.55%	0.054605	0.027302	12.93	0.003
Drilling Time	2	0.255177	58.63%	0.255177	0.127588	60.43	0.000
Abrasive Flow Rate * Water Jet Pressure	4	0.008131	1.87%	0.008131	0.002033	0.96	0.478
Abrasive Flow Rate * Drilling Time	4	0.004619	1.06%	0.004619	0.001155	0.55	0.707
Water Jet Pressure * Drilling Time	4	0.002885	0.66%	0.002885	0.000721	0.34	0.843
<b>Error</b>	8	0.016891	3.88%	0.016891	0.002111		
<b>Total</b>	26	0.043525	100.00%				

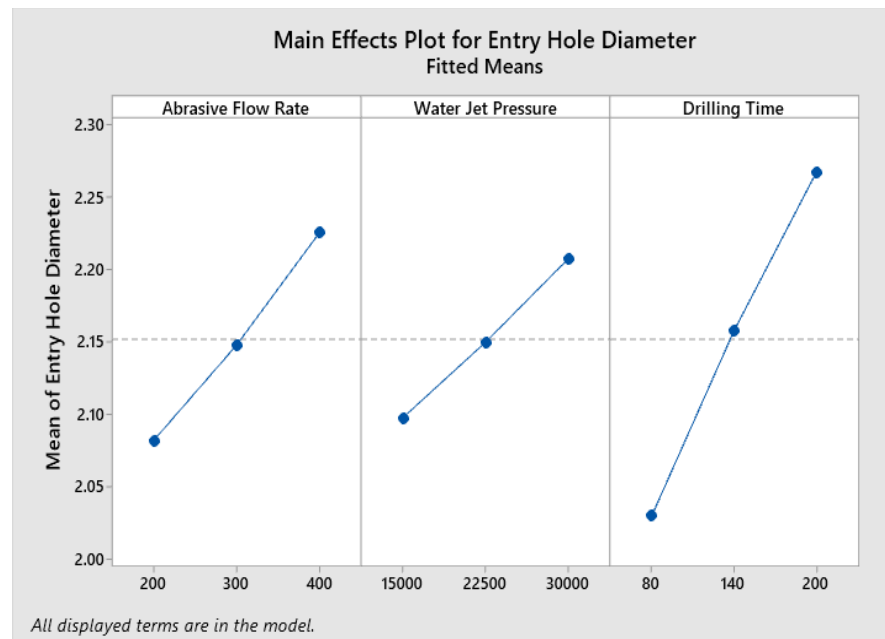


**Figure 2 Main Effects Plot for Entry Hole Diameter**

The regression equation is an algebraic equation which determines the relationship between the input parameters and the output parameters. For entry hole diameter, it was found that mass flow rate, water jet pressure and drilling time was found to be statistically significant and was to be included in the regression equation. Whereas, the interaction between the input parameters were not significant and hence they were excluded. The regression equation along with the coefficients was obtained with the help of Minitab software. The regression equation for entry hole diameter is as follows:

$$\text{Entry Hole Diameter} = a + b(\dot{m}) + c(P) + d(t) + \varepsilon \quad (1)$$

where,

Constant,  $a = 1.52$

Regression Coefficients,  $b = 0.000718$

$c = 0.000007$

$d = 0.001982$

$\varepsilon$  = Error

$\dot{m}$  is Abrasive Flow Rate,  $P$  is Water Jet Pressure,  $t$  is Drilling Time

The values of entry hole diameter which was measured with the help of profile projector was compared with the values calculated with the help of the regression equation. The comparison between the two values and the error is calculated and is as shown in the table

5. As the analysis was done at 95 % confidence level and there were other factors affecting the entry hole diameter such as dimensions of orifice and focusing nozzle, variation in size of abrasives used in the waterjet, the errors obtained is in the acceptable limit. Hence, the obtained regression equation is deemed as fit and can be used to predict the values of entry hole diameter for different values of Abrasive Flow Rate, Water Jet Pressure, Drilling Time other than the experimental values.

**Table 5 Error Analysis of regression equation for Entry Hole Diameter**

Hole No.	Experimental Value	Calculated Value	Percentage Error
1	1.909	1.927	0.94
2	2.024	2.046	1.08
3	2.136	2.165	1.34
4	1.957	1.980	1.14
5	2.078	2.099	0.98
6	2.184	2.218	1.51
7	2.044	2.032	0.58
8	2.124	2.151	1.26
9	2.282	2.270	0.53
10	1.942	1.999	2.85
11	2.125	2.118	0.34
12	2.191	2.237	2.05
13	2.035	2.051	0.80
14	2.110	2.170	2.78
15	2.251	2.289	1.67
16	2.090	2.104	0.66
17	2.194	2.223	1.30
18	2.393	2.342	2.19
19	2.108	2.071	1.80
20	2.191	2.190	0.06
21	2.253	2.309	2.41
22	2.068	2.123	2.60
23	2.263	2.242	0.93
24	2.404	2.361	1.82
25	2.115	2.176	2.79
26	2.313	2.295	0.80
27	2.315	2.414	4.09

### 3.2 Measurement of Cylindricity

The cylindricity is a method of measurement which determines the closeness of a drilled hole to a true cylinder. It was measured using a Coordinate Measuring Machine Contura G2 supplied by ZEISS 3D CNC. The cylindricity was measured with the positive tolerance kept constant at 0.1 mm. The deviation was measured using CMM and was tabulated as

shown in Table 3. The graphical representation of cylindricity deviation is as shown in Figure 3.

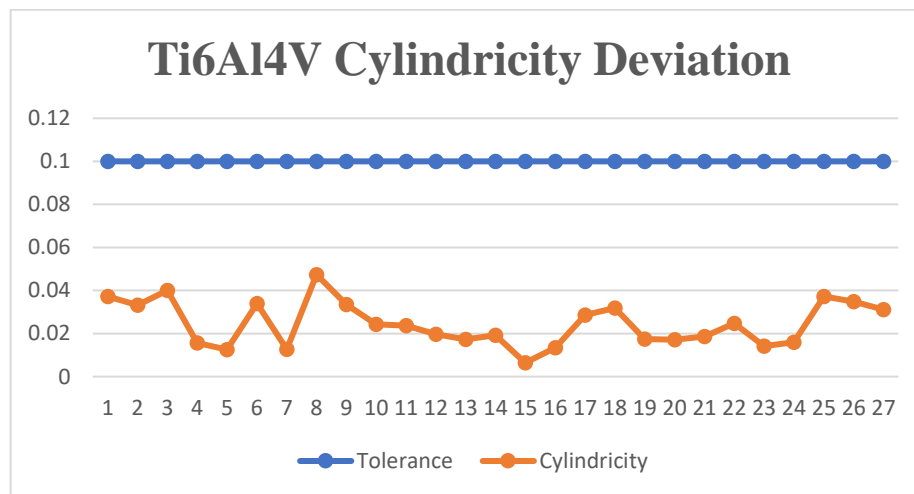


**Figure 3 Cylindricity Deviation for Ti6Al4V**

It was found that deviations measured for each hole was within the tolerance limit of 0.1 mm and with the help the graph it can be seen that the drilled holes behave as true cylinders.

### 3.3 Measurement of Hole Depth

To measure the hole depth, a vernier height gauge with a least count of 0.02 mm was used. The hole depth was tabulated and is as shown in Table 3. The front view of the workpiece after drilling 27 holes is as shown in figure 4. The workpiece was cut across center of each row of holes so as to view the hole profile of the drilled holes. The cross-sectional view of the workpiece is as shown in figure 4. The hole depth was measured using these cross-sectional cuts.

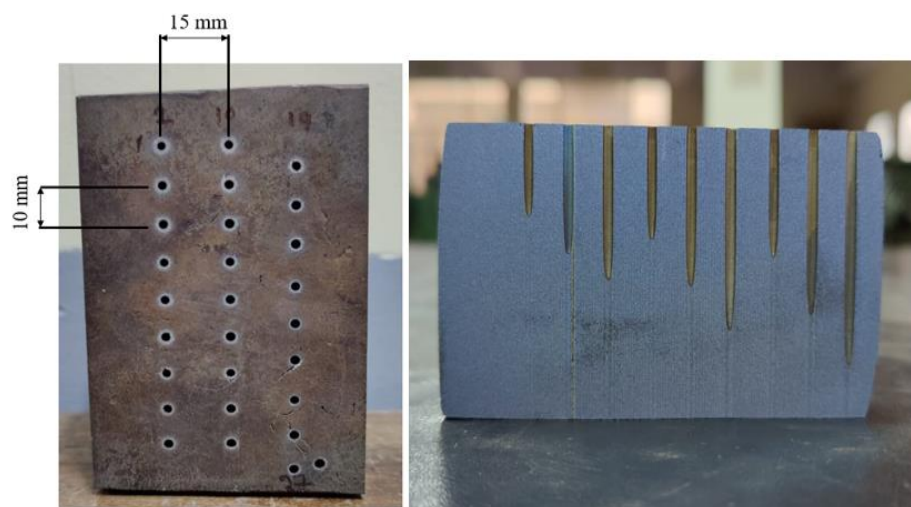


**Figure 4 Front View and Cross Sectional View of the workpiece**



In AWJ drilling, the hole produced is substantially wider than the jet stream, due mostly to the additional wall erosion resulting from the forceful upward ejection of the jet out of the blind cavity. The annular backflow region surrounding the incoming jet presents a highly turbulent and chaotic flow situation. The ejected stream is a churning mixture of water and air, laden with both shattered and intact abrasive particles as well as fragments of removed material. It interacts with both the incoming flow and the irregular, continuously evolving cavity surface. The abrasive water jet is stopped after the drilling time reaches the desired value in each trial which leads to formation of a blind hole. Hence as per the explanation given, the end of the blind hole takes the shape of a cone.

ANOVA was performed to determine the significant factors among AFR, WJP, DT and a regression equation was modelled to predict the effect of process parameters on hole depth. The ANOVA table for hole depth is as shown in Table 6. From the ANOVA table it can be observed that:

The F-ratios presented in the table 6 for Abrasive Flow Rate, Water Jet Pressure and Drilling Time are more than F-ratios given in the statistical tables. Further, the P-values obtained from the ANOVA analysis for these parameters are less than 0.05. Therefore, it can be concluded that these parameters are most statistically significant parameters influencing the hole depth. Further, the interaction effects are not significant as their P-values are greater than 0.05.

**Table 6 ANOVA Table for Hole Depth**

Source	DF	Seq SS	Contribution	Adj SS	Adj MS	F-Value	P-Value
Abrasive Flow Rate	2	114.28	7.87%	114.28	57.141	129.33	0.000
Water Jet Pressure	2	368.43	25.38%	368.43	184.216	416.93	0.000
Drilling Time	2	910.61	62.74%	910.61	455.307	1030.49	0.000
Abrasive Flow Rate * Water Jet Pressure	4	10.89	0.75%	10.89	2.722	6.16	0.015
Abrasive Flow Rate * Drilling Time	4	7.87	0.54%	7.87	1.968	4.45	0.035
Water Jet Pressure * Drilling Time	4	35.87	2.47%	35.87	8.967	20.29	0.000
<b>Error</b>	8	3.53	0.24%	3.53	0.442		
<b>Total</b>	26	1451.49	100.00%				

The contribution of abrasive flow rate (A), water jet pressure (B) and drilling time (C) on hole depth was found to be 7.87 %, 25.38 %, 62.74 % respectively. The total contribution of abrasive flow rate, waterjet pressure and drilling time amounts to around 96% on hole depth. Percentage contribution of interactions, that is, abrasive flow rate and waterjet pressure, abrasive flow rate and drilling time, waterjet pressure and drilling time adds up to around 3.7%, and the interaction effects are significant and is to be included in the regression equation. The percentage error around 0.24 % indicates the contribution of other parameters such as dimensions of orifice and focusing nozzle, variation in size of abrasives used in the waterjet and etc. on the hole depth. The interaction of abrasive flow rate, waterjet pressure and drilling time (ABC) is not considered in ANOVA. The main effect plots for hole depth is as shown in figure 5. The following inferences can be made from the graph: The hole depth was found to increase with increase in abrasive flow rate. This is due to the fact that a greater number of abrasive particles participate in eroding the target material as the abrasive flow rate increases. The hole depth was found to increase with increase in water jet pressure. With increase in water jet pressure, the energy possessed by the jet is higher since the velocity of abrasive particles is very high. The hole depth was found to increase with increase in drilling time. This is due to the fact that abrasive particles participating in erosion are in contact with the target material for longer duration as the drilling time increases.

The regression equation is an algebraic equation which determines the relationship between the input parameters and the output parameters. For hole depth, it was found that mass flow rate, water jet pressure and drilling time was found to be statistically significant and was to be included in the regression equation. The interactions between the input parameters, that is, mass flow rate & water jet pressure (A&B), mass flow rate & drilling time (A&C), water jet pressure & drilling time (B&C) were also found to be significant and hence they were also included. Since the interactions were found to be significant, they were included in the regression equation. As the individual terms and the interactions were to be included in the regression equation, a quadratic equation involving both the individual and the interaction terms was formulated. The regression equation along with the regression coefficients was obtained with the help of Minitab software. The regression equation for hole depth is as follows:

$$\text{Hole Depth} = a + b(\dot{m}) + c(P) + d(t) + e(\dot{m}^2) + f(P^2) + g(t^2) + h(\dot{m}P) + i(\dot{m}t) + j(Pt) \quad (2)$$

where,

a	b	c	d	e	F	g	h	i	j
5.19	0.0064	0.000011	0.0523	0.000025	0.000001	0.000195	0.000001	0.000131	0.000004

m is Abrasive Flow Rate, P is Water Jet Pressure, t is Drilling Time

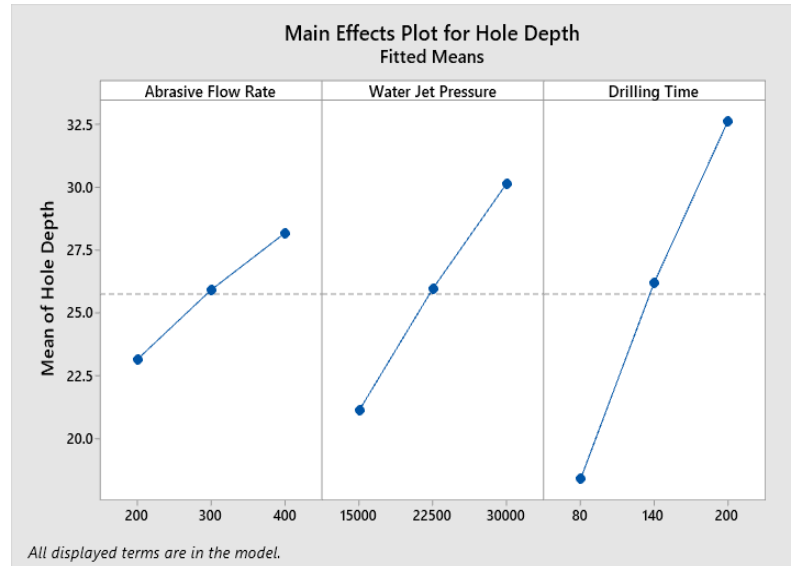


**Figure 5 Main Effects Plot for Hole Depth**

The values of hole depth which was measured with the help of vernier height gauge was compared with the values calculated with the help of the regression equation. The comparison between the two values and the error is calculated and is as shown in the table 7. As the analysis was done at 95 % confidence level and there were other factors affecting the hole depth such as dimensions of orifice and focusing nozzle, variation in size of abrasives used in the waterjet, the errors obtained is in the acceptable limit. Hence, the obtained regression equation is deemed as fit and can be used to predict the values of hole depth for different values of Abrasive Flow Rate, Water Jet Pressure, Drilling Time other than the experimental values.

**Table 7 Error Analysis of regression equation for Hole Depth**

<b>Hole No.</b>	<b>Experimental Value</b>	<b>Calculated Value</b>	<b>Percentage Error</b>
1	14.16	14.26	0.70
2	21.20	20.94	1.24
3	23.16	22.54	2.75
4	16.58	16.60	0.12
5	23.06	22.46	2.67
6	30.08	29.88	0.67
7	19.32	19.42	0.51
8	26.76	26.84	0.30
9	34.04	33.92	0.35
10	15.02	15.08	0.40
11	22.16	22.42	1.16
12	26.84	27.01	0.63
13	18.74	17.96	4.34
14	25.90	26.22	1.22
15	33.74	32.64	3.37
16	21.36	22.08	3.26
17	31.00	30.96	0.13
18	38.50	38.30	0.52
19	16.58	16.22	2.22
20	23.38	23.12	1.12
21	27.56	27.24	1.17
22	20.18	21.02	4.00
23	29.12	28.96	0.55
24	36.38	35.91	1.31
25	23.80	23.64	0.68
26	33.38	32.88	1.52
27	43.26	44.04	1.77

### 3.4 Scanning Electron Microscope

The Scanning Electron Microscope (SEM) images reveal the erosion behavior of holes drilled in Ti6Al4V. The SEM images of holes with minimum, mean, maximum depth is as shown in figures 6, 8, 9.

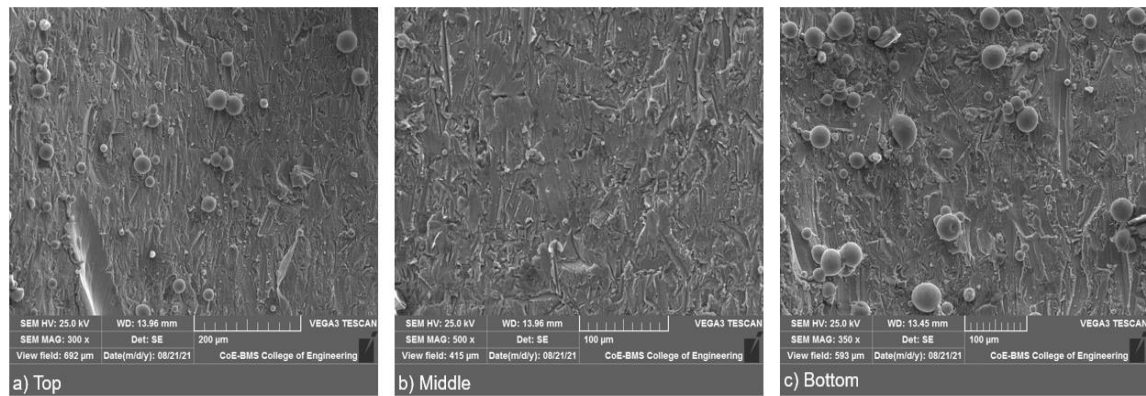


**Figure 6 SEM images of hole drilled with Abrasive flow rate at 200 g/min, Water jet pressure at 15000 psi, drilling time at 80 seconds (Minimum Hole Depth)**

In order to determine the chemical composition of the sample with minimum hole depth, Energy Dispersive X-Ray Analysis (EDS or EDX) was used which gives the distribution as shown in figure 7 and concentration of the elements in the sample as shown in table 8.

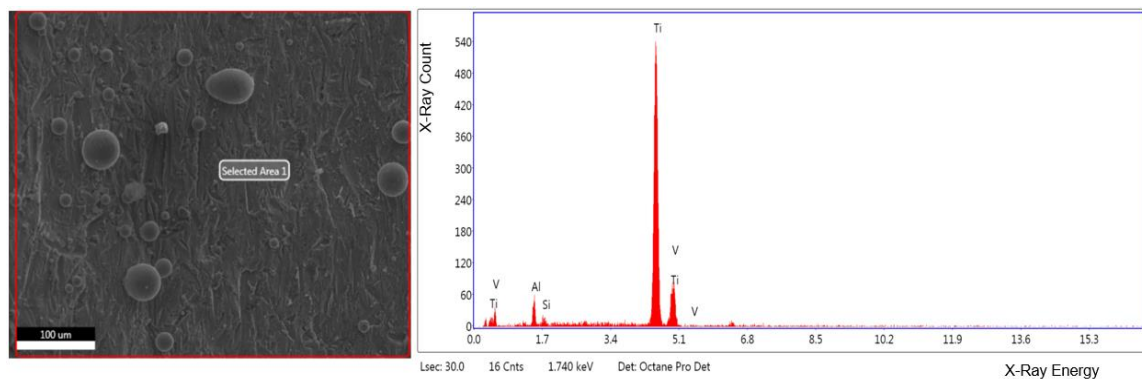


**Figure 7 EDX spectrum of hole with maximum hole depth**

**Table 8 EDX analysis results of hole with maximum hole depth**

Element	Shell	Weight %
Al	K	5.52
Si	K	1.42
Ti	K	88.16
V	K	4.90

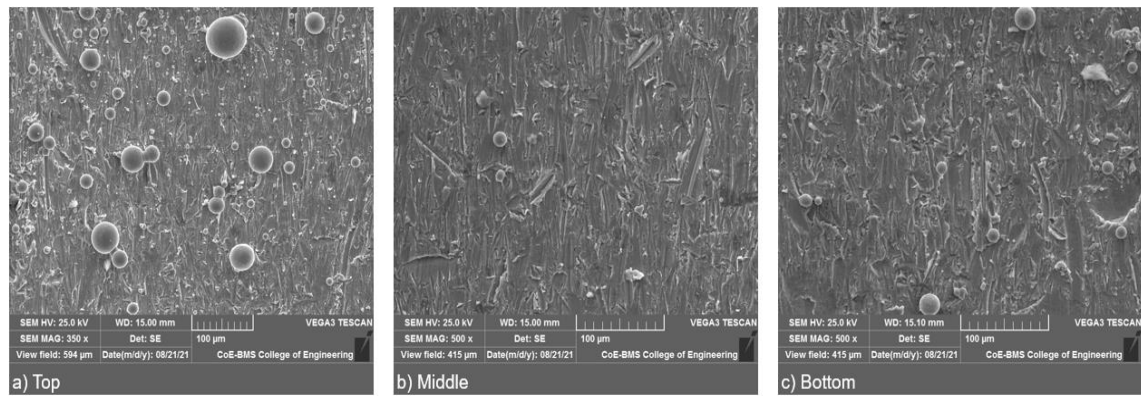


**Figure 8 SEM images of hole drilled with Abrasive flow rate at 300 g/min, Water jet pressure at 15000 psi, drilling time at 200 seconds (Intermediate Hole Depth)**

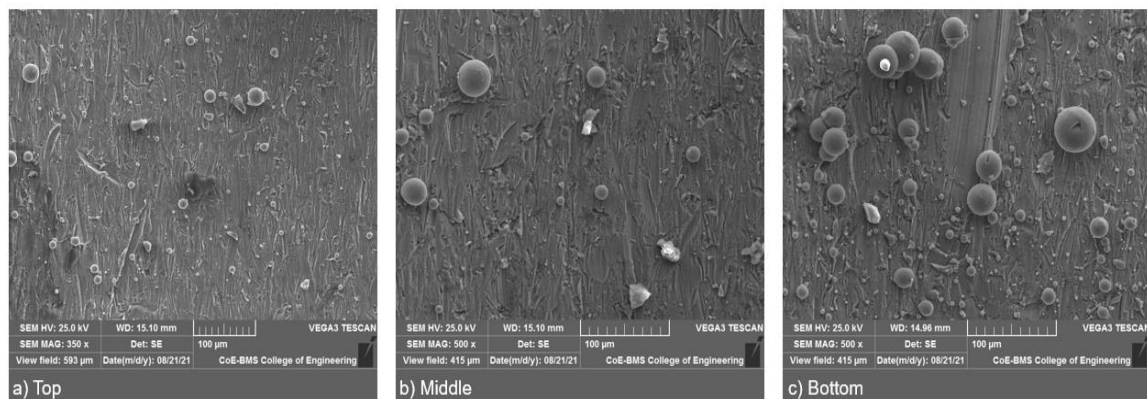


**Figure 9 SEM images of hole drilled with Abrasive flow rate at 400 g/min, Water jet pressure at 30000 psi, drilling time at 200 seconds (Maximum Hole Depth)**

In order to determine the chemical composition of the sample with maximum hole depth, Energy Dispersive X-Ray Analysis (EDS or EDX) was used which gives the distribution as shown in figure 10 and concentration of the elements in the sample as shown in table 9.

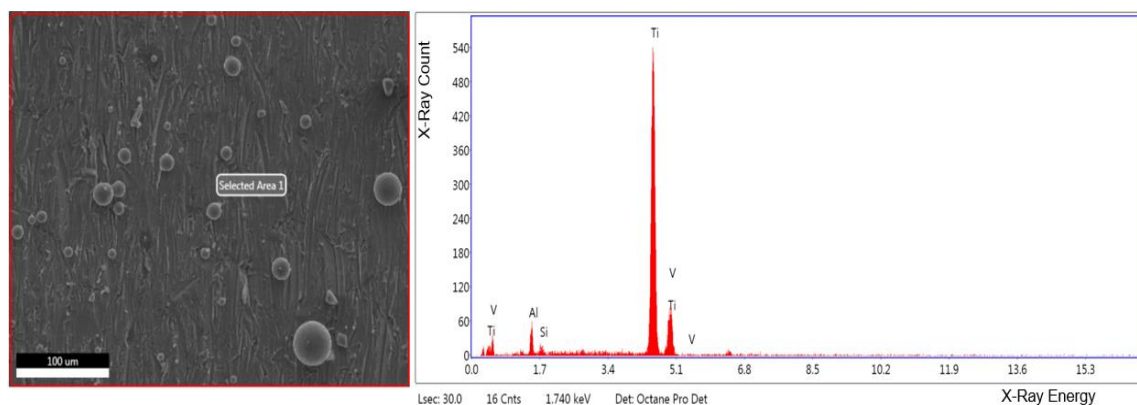


**Figure 10 EDX spectrum of hole with maximum hole depth**

**Table 9 EDX analysis results of hole with maximum hole depth**

Element	Shell	Weight %
Al	K	5.38
Si	K	1.06
Ti	K	88.15
V	K	5.41

### 3.4.1 Observations from SEM and EDX analysis

The SEM images of three different drilled holes are as shown in the figure 6, 8 and 9. The observations from the SEM and EDX analysis are as follows:

- From figure 6 (a), 6 (b), 6 (c) it was seen that the eroded surface was very rough and the eroded particles are not in uniform in their shape and size.
- The metal substrate was analysed using Energy Dispersive X-Ray Analysis to determine the weight percentage of each element and was found that Titanium, Aluminium and Vanadium had higher weight percentages as seen in table 8. This is due to the fact that when material is removed by abrasive water jet, due to raise in localized temperatures in some areas, the eroded particles are adhered to the substrate.
- The Silica element found in the EDX analysis is found to have the weight percentage of around 1.06%. This is because 98.5% of the abrasive particles entrained in the water jet participate in the material removal and that energy is harnessed to cut the material. About 1.5% do not participate in the erosion mechanism and are lodged on the surface as their kinetic energy is less to cut the material. This residue is reflected in the EDX analysis.
- The SEM images and EDX analysis of the intermediate hole depth and maximum hole depth are as shown in figure 8 (a), 8 (b), 8 (c) & 9 (a), 9 (b), 9 (c) and figure 10 respectively. The same trend was seen in the SEM images of intermediate hole depth and maximum hole depth.

## 4. Conclusions

Abrasive Water Jet Drilling, a non-traditional machining technique was used to drill Ti6Al4V and was performed based on the experiments designed according to Taguchi method. The conclusions that can be drawn from analysis of the hole profile are as follows:

---

Entry Hole Diameter was found to increase with increase in input parameters, that is, abrasive flow rate, water jet pressure, drilling time based on ANOVA results. It was not significantly affected by the interactions between the input parameters and hence was neglected in the formulation of regression equation. Cylindricity was measured for all the 27 holes and it was found that all the holes were within the tolerance limit of 0.1 mm. If the tolerance limit is within 0.025 mm, the deviations obtained in this study does not adhere to it. Hence, for accurately drilling of hole with tolerance limit less than 0.025 mm, abrasive water jet drilling cannot be used for this material. Hole depth was found to increase with increase in input parameters, that is, abrasive flow rate, water jet pressure, drilling time based on ANOVA results. It was significantly affected by the interactions between the input parameters and hence was included in the formulation of regression equation. The SEM images of three different drilled holes are as shown in the images above and the eroded surface is found to be very rough and the eroded particles are not in uniform in their shape and size and when analysed using Energy Dispersive X-Ray Analysis it was found that Titanium, Aluminium and Vanadium had higher weight percentages. This is due to the fact that when material is removed by abrasive water jet, due to raise in localized temperatures in some areas, the eroded particles are adhered to the substrate. The silica elements found during EDX analysis is due to the residue of abrasive particles.

This research work can be used as a data bank in machining industries for applications such as marine industries where drilling of Ti6Al4V is necessary. There is scope for further study where these experimental results can be validated using Finite Element Analysis. It can also be referred for a study where an empirical and analytical model can be developed to obtain the relationship between input parameters and output parameters such as entry hole diameter and hole depth.



---

**References**

- [1] Jegaraj JJR, Babu NR, 2007, “A soft computing approach for controlling the quality of cut with abrasive water jet cutting system experiencing orifice and focusing to wear”, *J Mater Process Technol*, 185, pp. 217-227.
- [2] Li, H., Wang, J. An experimental study of abrasive waterjet machining of Ti-6Al-4V. *Int J Adv Manuf Technol* 81, 361–369 (2015).
- [3] LiW,Wang J, Zhu H, Li H, Huang C (2013) On ultrahigh velocity micro-particle impact on titanium—a single impact study. *Wear* 35(1–2):216–227.
- [4] Caydas U, Hascalik A, 2008, “A study on surface roughness in abrasive water jet machining process using Titanium Alloy and regression analysis method”, *J Mater Process Technol*, 202, pp. 574-582.
- [5] S.M. Afazova, R. Ronaldo, D. Lonsdale, D. Zdebski, S.M. Ratchev, “Analysis of micro-drilling of glassy ceramic Macor nozzles for scanning droplet systems”, *Journal of Materials Processing Technology* 213 (2013) 221–228.
- [6] Alberdi A, Artaza T, Suarez A, Rivero A, Girot F. An experimental study on abrasive waterjet cutting of CFRP/Ti6Al4V stacks for drilling operations. *Int J Adv Manuf Technol* 2016;86(1-4):691–704.
- [7] Escobar-Palafox GA, Gault R, Ridgway K. Characterisation of abrasive water-jet process for drilling titanium and carbon fibre reinforced polymer stacks. *Surfaces* 2012;13:14.
- [8] Chang CW, Kuo CP, 2007, “Evaluation of surface roughness in laser-assisted machining of Titanium oxide ceramics with Taguchi method”, *Int J Mach Tool Manuf*, 47, pp. 141-147.

## PLAGIARISM REPORT

"Abrasive water jet drilling of Titanium and analysis of hole profile"

### ORIGINALITY REPORT

<b>17</b> %	<b>6</b> %	<b>13</b> %	<b>5</b> %
SIMILARITY INDEX	INTERNET SOURCES	PUBLICATIONS	STUDENT PAPERS

### PRIMARY SOURCES

<b>1</b>	Rodney R. Boyer. "Titanium and Its Alloys: Metallurgy, Heat Treatment and Alloy Characteristics", Wiley, 2010 Publication	<b>3</b> %
<b>2</b>	S. Srinivas, N. Ramesh Babu. "PENETRATION ABILITY OF ABRASIVE WATERJETS IN CUTTING OF ALUMINUM-SILICON CARBIDE PARTICULATE METAL MATRIX COMPOSITES", Machining Science and Technology, 2012 Publication	<b>1</b> %
<b>3</b>	Kapil Gupta, Neelesh Kumar Jain, Rudolph Laubscher. "Advances in Gear Manufacturing", Elsevier BV, 2017 Publication	<b>1</b> %
<b>4</b>	<a href="http://www.azom.com">www.azom.com</a> Internet Source	<b>1</b> %
<b>5</b>	<a href="http://www.slideshare.net">www.slideshare.net</a> Internet Source	<b>1</b> %
<b>6</b>	Mahesh ShivajiRao, Srinivas Satyanarayana. "Abrasive water jet drilling of float glass and	<b>1</b> %